Available online at www.sciencedirect.com
SCIENCE DIRECT®
Deep-Sea Research I 50 (2003) 1157–1187
DEEP-SEA RESEARCH PART I
www.elsevier.com/locate/dsr

Transient physical forcing of pulsed export of bioreactive material to the deep Sargasso Sea

M.H. Conte[a,*], T.D. Dickey[b], J.C. Weber[a], R.J. Johnson[c], A.H. Knap[c]

[a] *Department of Marine Chemistry and Geochemistry, Woods Hole Oceanographic Institution, 360 Woods Hole Road, MS 25, Woods Hole, MA 02543, USA*

[b] *Ocean Physics Laboratory, University of California, Santa Barbara, 6487 Calle Real Unit A, Santa Barbara, CA 93117, USA*

[c] *Bermuda Biological Station for Research, Inc., Ferry Reach, St. Georges GE01, Bermuda*

Received 23 August 2002; received in revised form 26 March 2003; accepted 1 August 2003

Abstract

Considerable attention has recently been focused on the role of eddies in affecting biogeochemical fluxes and budgets of the Sargasso Sea. In late November 1996, the Bermuda Testbed Mooring (BTM) and Bermuda Atlantic Time Series (BATS) shipboard sampling evidenced a fall phytoplankton bloom at the Bermuda time-series site which was strongly forced by the interplay between seasonal mixed layer destratification and perturbation of mixed layer dynamics due to passage of a warm mesoscale feature. The feature was characterized by clockwise current vector rotation from near the surface to about 200 m and a thick, warm, low salinity isothermal layer >180 m in depth. Nutrients, chlorophyll fluorescence and pigment profiles indicated high primary production stimulated by enhancement of nutrient entrainment and intermittent deep mixing down to the base of the feature's isothermal layer. Nearly coincident with the arrival of this productive feature at the BTM site, the Oceanic Flux Program (OFP) sediment traps recorded an abrupt, factor of 2.5 increase in mass flux at 3200 m depth. Even more dramatic was the observed increase in flux of labile bioreactive organic matter. Fluxes of primary phytoplankton-derived compounds increased by factors of 7–30, bacteria-derived compounds by 6–9, and early degradation products of sterols by a factor of 10. The covariation of early degradation products and bacteria-derived compounds with phytoplankton-derived compounds indicated that the settling phytoplankton bloom material contained elevated bacterial populations and was undergoing active degradation when it entered the 3200 m trap cup.

The increase in the flux of bulk components, especially the residual silicate fraction, and refractory organic compounds clearly preceded the main pulse of the labile, surface-derived phytoplankton organic material. The coincident increase in the flux of refractory and zooplankton-derived compounds suggests that in the initial stage of the deep flux event, the mass flux increased largely as a result of an increase in the flux of refractory materials scavenged from the water column and repackaged into sinking particles and increased zooplankton inputs. These results imply that biological reprocessing of flux material within the water column acts to enhance the coupling between the surface and deep ocean environments.

Our results show that transient, upper ocean forcing associated with variable upper ocean physical structure—which includes but is not limited to eddies—and variable meteorological forcing can have an enormous effect on the export flux of bioreactive organic material. The importance of pulsed fluxes of bioreactive material arising from transient physical forcing to the long-term average is not presently known. However, the occurrence of episodic high flux events throughout the OFP time-series record (also inferred from BTM time-series) suggests that such forcing, regardless of

*Corresponding author. Fax: +1-508-457-2193.
E-mail address: mconte@whoi.edu (M.H. Conte).

0967-0637/$ - see front matter
doi:10.1016/S0967-0637(03)00141-9

specific dynamics, may be responsible for a significant fraction of the total export flux of bioreactive carbon and associated elements to the deep oligotrophic ocean.

Keywords: Particle flux; Lipids; Bermuda; Mesoscale variability; Moorings; Pigments

1. Introduction

Variability in space and time is an inherent property of the ocean—climate system. Time-series observations have revealed variability in upper ocean biogeochemical parameters over a number of time scales (e.g., the Continuous Plankton Recorder time-series [e.g., Dickson et al., 1996], the California CalCOFI time-series [e.g., Chelton et al., 1982], the US-JGOFS Bermuda Atlantic Time Series (BATS) [e.g., Steinberg et al., 2001], the Bermuda Testbed Mooring (BTM) [e.g., Dickey et al., 1998a, 2001], and the Hawaii Ocean Time-series (HOT) [e.g., Karl et al., 2001]). Causal factors on some scales (e.g., daily, lunar, annual) are comparatively well understood, but the causes of much of the observed non-seasonal variability remains enigmatic. Meteorological and physical forcing appears to drive abrupt short-term changes in ocean properties which occur on time scales of days–weeks (e.g., Platt et al., 1989; Chavez and Smith, 1995; Dickey et al., 1994, 1998a, b, c, 2001; Marra et al., 1998; McNeil et al., 1999). Williams and Follows (2002) and Lewis (2002) have recently completed comprehensive reviews of mechanisms that affect physical transport of nutrients and their roles in maintaining biological production.

Variability on short (less than a day–weeks) time scales also exists in the export of material and energy to the deep ocean (e.g., Deuser, 1986; Granata et al., 1995; Newton et al., 1994; Fischer et al., 1996; Karl et al., 1996; Ratmeyer et al., 1999; Honjo et al., 1999; Conte et al., 2001a). In the northern Sargasso Sea, the 24 + year Oceanic Flux Program (OFP) sediment trap time-series provided the first direct evidence of a seasonal variation in the deep ocean fluxes that was directly tied to the seasonal variations in overlying surface water productivity (Deuser et al., 1981, 1990; Deuser, 1986). Since that time, the higher resolution biweekly resolved flux record has also clearly identified large changes in deep ocean fluxes on < monthly time scales (Conte et al., 2001a). In particular, episodic and abrupt short-lived changes in mass flux are a persistent feature of the time-series record. Similar evidence for short-lived pulses in flux to the deep ocean has been identified in the North Atlantic (Billett et al., 1983; Lampitt, 1985), the eastern Atlantic (Fischer et al., 1996), and the Arabian Sea (Dickey et al., 1998b; Marra et al., 1998; Honjo et al., 1999).

Non-seasonal short-lived flux events can greatly enhance the flux of labile biogenic material to the deep ocean (Conte et al., 1998a). The nature of short-lived change in flux quantity and quality may, in turn, be a critical factor determining the vertical penetration depths of nutrients and easily remineralized elements and the temporal patterns of food supply for midwater and benthic organisms (Rice et al., 1986; Graf, 1989; Gooday and Turley, 1990; Pfannkuche, 1993; Gehlen et al., 1997; Smith et al., 1996, 2002).

At the Bermuda time-series site, an influence of physical forcing on mixed layer dynamics and on non-seasonal, short-lived variability in deep ocean particle fluxes is implicated by the observations that extreme mass fluxes are episodic yet most frequent during the early winter and late spring periods of destratification and stratification, not during the period of highest mean flux, and secondly, that these same periods also exhibit the largest interannual variability in flux (Conte et al., 1998a, 2001a). The inferences from these observations are that transient, physically forced perturbations in the surface mixed layer—such as the advection of mesoscale eddies and water masses having differing physical dynamics and the passage of synoptic-scale weather systems (i.e., high and low pressure systems of 1001–2500 km

scale)—affect upper ocean biology and generate conditions favoring enhanced surface export flux (e.g., McGillicuddy et al., 1998; McNeil et al., 1999; Dickey and Falkowski, 2002; Sweeney et al., in press). Evidence for a direct coupling between transient, physical features and deep ocean flux has been observed in the Arabian Sea (Dickey et al., 1998b; Honjo et al., 1999), where a large increase in deep mass flux was associated with an eddy with observed high biomass and primary productivity in the overlying upper ocean waters.

The collaborative integration of three complementary time-series observational programs in deep waters off Bermuda—the OFP sediment trap time-series, the BATS and the BTM—now allows us to examine the connections between upper ocean physical processes and export flux to the deep ocean. In this paper, we describe a pulsed export event in the 3200 m OFP flux record that was strongly forced by the interplay between wind forcing and seasonal destratification and transient changes in mixed layer dynamics associated with the advection of a warm, low salinity mesoscale feature. While the data are not sufficient to fully characterize the feature, they clearly show that perturbation of mixed layer dynamics by mesoscale physical features plays a very significant role in generating conditions that favor pulsed export of labile, bioreactive materials to the deep ocean.

2. Background

2.1. Description of the Bermuda time-series site and research programs

The oceanographic setting of the Bermuda time-series site has been summarized by Michaels and Knap (1996), Joyce and Robbins (1996), Conte et al. (2001a), Dickey et al. (1998a, 2001) and Steinberg et al. (2001). The site is located in ~4500 m of water at the northern edge of the Sargasso Sea subtropical gyre in a transition zone between relatively eutrophic waters to the north and oligotrophic subtropical waters to the south. Synoptic-scale weather patterns typically pass every few days and hurricanes every few years or sometime more frequently (e.g., Dickey et al., 1998a, c, 2001). Major variations in mixed layer depth can occur on the order of days during winter and spring (Dickey et al., 1998a, 2001). These are driven by surface heating countered by intense wind mixing and possibly convection associated with cold, dry air periods.

Weak surface fronts and energetic submesoscale and mesoscale features often pass through the region and affect locally observed biology (Dickey et al., 1998a, 2001; Granata et al., 1995; McGillicuddy et al., 1998, 1999, 2001; McNeil et al., 1999; Siegel et al., 1999). Mesoscale eddies and submesoscale features may enhance nutrient upwelling and mixing and overall appear to enhance biological productivity (McGillicuddy and Robinson, 1997; McGillicuddy et al., 1998, 2001; Oschlies and Garçon, 1998; Siegel et al., 1999; Williams and Follows, 2002; Lewis, 2002), although direct observational evidence is limited (McNeil et al., 1999; Garçon et al., 2001; Sweeney et al., in press).

The first sustained time-series program off Bermuda was Hydrostation S (32°10′N, 64°30′W), a time-series of biweekly measurements of physical and chemical properties in the upper 4200 m (see Joyce and Robbins, 1996; Michaels and Knap, 1996 for review). The OFP sediment trap time-series was initiated in 1978 near Hydrostation S (see Deuser, 1996; Conte et al., 2001a for review). The OFP time-series, presently located at 31°50′N, 64°10′W, continuously samples particle flux at 500, 1500 and 3200 m with a nominal 2-week sampling resolution. The surface catchment area of the 3200 m trap is at the mesoscale and on the order of 10^5–10^6 km^2 for particles with a settling velocity at 100 m d^{-1} (Siegel and Armstrong, 2002). The US JGOFS BATS study began ~monthly measurements of upper ocean physical and biogeochemical properties near the OFP site in 1988 (Michaels and Knap, 1996; Steinberg et al., 2001). The present BATS sampling location is nominally at 31°40′N, 64°10′W. Surface export flux measured by BATS during 3-day drifting trap deployments is highly correlated with the continuous OFP flux record, and indicates that upper ocean conditions measured at the BATS site are representative of the larger, mesoscale "statistical funnel" sampled by the deep traps (Conte et al., 2001a).

The BTM (Dickey et al., 1998a, 2001) was first deployed in 1994 and is located midway between the OFP and BATS sites. For the period of this study, the BTM mooring was located at 31°44′N, 64°10′W. The BTM makes high temporal resolution meteorological, physical (currents, temperature, and salinity) and bio-optical (chlorophyll fluorescence, multi-spectral downwelling/upwelling radiance, photosynthetically available radiation) measurements within the upper 200 m. BTM data are available at www.opl.ucsb.edu.

Regional satellite studies provide a mesoscale context for the in situ observations. These have included studies of sea-surface temperature and near-surface color (Nelson, 1998; Glover et al., 2002) and mesoscale eddy fields (McGillicuddy et al., 2001). McGillicuddy and Kosnyrev (2001) have recently developed a three-dimensional ocean model of mesoscale eddy fields for the OFP/BTM/BATS area using Topex/Poseidon and European Resource Satellite (ERS) altimetry data which covers the period of this study.

2.2. Diagnostic lipid biomarkers in trap material

Over a hundred extractable lipid compounds are present in oceanic particulate matter. Although the precise origins of many compounds remain unknown, current knowledge of taxonomic distributions and diagenetic transformations allows inferences to be made about organic matter sources and lability (i.e., "freshness" or ease of degradability).

Table 1 lists the diagnostic "biomarker" compounds used in this study. Several compound classes, such as the $C_{37–39}$ alkenones of the coccolithophore *Emiliania huxleyi* and other closely related prymnesipohytes (reviewed in Conte et al., 1994) and the mid-chain diols and hydroxy acids of eustimatophytes (Volkman et al., 1992; Gelin et al., 1997; Versteegh et al., 1997) are specific to particular phytoplankton taxa. Other compound classes, such as $C_{27–30}$ sterols (Volkman, 1986; Barrett et al., 1995; Volkman et al., 1998) and $C_{18–22}$ polyunsaturated fatty acids (PUFAs, Harwood and Russell, 1984) are synthesized by many phytoplankton groups, but often have taxonomically distinct distributions. For example, diatoms generally contain predominately C_{16} and 20:5ω3 PUFAs, whereas most prymnesiophytes and dinoflagellates contain predominately C_{18} and 22:6ω3 PUFAs (Harwood and Russell, 1984).

As organic matter cycles through the food web, the residual matter becomes progressively more enriched in resistant compounds and transformation products characteristic of heterotrophic alterations and new compounds that synthesized de novo by microbes and animals are introduced (reviewed in Wakeham and Lee, 1993). Bioreactive, labile compounds such as PUFAs and some sterols are remineralized or bioassimilated and may be subsequently altered (reviewed in Bradshaw and Eglinton, 1993). For example, C_{28} and C_{29} sterols are dealkylated and/or hydrogenated to produce cholesterol and stanols (e.g., Teshima and Kanazawa, 1972; Ikekawa, 1985). Typically, animal biomass is enriched in PUFAs, cholesterol, 18:1ω9, and compounds (e.g., the $C_{14–18}$ *n*-alkanols of wax ester synthesizing animals) originating from de novo biosynthesis (Sargent and Whittle, 1981; Saito and Murata, 1996). In contrast, fecal material is enriched in cholesterol, stanols, saturated and monounsaturated acids, and bacteria-derived compounds, but is extremely depleted in PUFAs. Compounds indicative of bacteria-derived carbon include odd and branched chained C_{12}–C_{19} acids, β and $\omega-1$ hydroxy acids (Perry et al., 1979; Parkes and Taylor, 1983; Gillan and Johns, 1986; Kaneda, 1991), and a series of $C_{29–33}$ hopanoic acids, alcohols, ketones and hopenes, which are degradation products of C_{35} bacteriohopanepolyols (Rohmer et al., 1984; Ourisson et al., 1987).

Highly reactive compounds and transformation products provide information about organic matter lability. PUFAs are a particularly useful indicator of organic matter lability, as these compounds have half-lives in oceanic detritus on the order of days (Conte, 1989). As fresh organic material is microbially degraded, there is an increase in concentrations of bacteria-derived compounds such as hydroxy acids (e.g., DeLeeuw et al., 1995) and an increase in the concentrations of degradation products such as steroidal ketones (Mermoud et al., 1984) and stanols (Bjorkhem and Gustaffson, 1971) relative to primary phytoplankton-derived compounds. The extractable lipids of

Table 1
Diagnostic lipid biomarkers in 3200 trap material and major sources

Lipid biomarker	Major source(s)	References
C_{14-22} saturated and monounsaturated *n*-acids (SAT, MONO)	Multiple sources although shorter chained acids predominate in phytoplankton and bacteria. 18:1ω9 is a major animal acid; 18:1ω7 is a major bacterial acid. Present in high concentrations in fecal material	Harwood and Russell (1984), Sargent (1976), and Bradshaw and Eglinton (1993)
C_{14-19} odd and branched saturated and monounsaturated acids (ODD/BR ACIDS)	Gram negative bacteria	Gillan and Johns (1986)
ω3 polyunsaturated fatty acids (PUFAs)	Phytoplankton-synthesized compounds bioaccumulated by zooplankton. Present in high concentrations in zooplankton biomass. Rapidly degraded in water column. Virtually absent in zooplankton fecal material. Barophilic bacteria may be a possible source	Sargent (1976), Prahl et al. (1984), Harvey et al. (1987), Conte (1989), Bradshaw and Eglinton (1993), Yano et al. (1997), and Fang et al. (2000)
$C_{27}\Delta^5$ and $\Delta^{5,22}$ sterols, $C_{28}\Delta^{5,22}$, $C_{29}\Delta^5$ and $\Delta^{5,22}$ sterols	Phytoplankton-synthesized compounds. $C_{28}\Delta^{5,22}$ is a major sterol in many coccolithophores and diatoms	Volkman (1986) and Volkman et al. (1998)
Choles-5-en-3β-ol (cholesterol)	Primarily biotransformation product of phytoplankton sterols. Minor phytoplankton synthesis (esp. dinoflagellates and eustigmatophytes) present in high concentrations in zooplankton biomass and in fecal material	Teshima and Kanazawa (1972), Ikekawa (1985), Volkman et al. (1998), Mansour et al. (1999), Sargent (1976), Wakeham and Canuel (1986), Bradshaw and Eglinton (1993), and Nelson et al. (2000)
Steroidal ketones	Early degradation products of sterols. Possible minor dinoflagellate source	Gagosian et al. (1980), Mermoud et al. (1984), Volkman et al. (1998), Wakeham (1987)
Stanols	Primarily bacterial dehydrogenation products of Δ^5 sterols. Abundant in fecal material. Minor phytoplankton source	Gaskell and Eglinton (1975) and Nishimura and Koyama (1977), Wakeham (1995)
C_{37-39} alkenones and alkyl alkenoates (LCK)	Phytoplankton-synthesized compounds. Open ocean synthesis restricted to the coccolithophores *Emiliania huxleyi* and *Geophyrocapsa* sp. Unsaturation ratio of alkenones closely controlled by growth temperature	Conte et al. (1994) and Bijma et al. (2001)
C_{28-30} alkan-1,15-diols + alkan-15-one-1-ols	Presumed phytoplankton-synthesized compounds	DeLeeuw et al. (1981)
C_{28-32} diols, ket-1-ols and mid-chain hydroxy acids	Presumed phytoplankton source. Identified in eustigmatophytes but synthesis by other classes is likely	Volkman et al. (1992) and Gelin et al. (1997), Versteegh et al. (1997)
1-0-Alkylglycerols	Alkyldiacylglycerols are abundant in sharks, squid and the pteropod *C. limacina*, and 1-0-alkylglycerols in shark. Also identified in sulfate-reducing bacteria, suggesting bacterial sources as well	Sargent (1989), Zeng (1988), Bordier et al. (1996), Phleger et al. (1997), Kattner et al. (1998)

Table 1 (*continued*)

Lipid biomarker	Major source(s)	References
C_{30-33} hopanols, hopanoic acids, hopanones and hopenes (HOPANOIDS)	Early degradation products of C_{35} bacteriohopanepolyols, including some cyanobacteria such as *Synechococcus*	Rohmer et al. (1984), Ourisson et al. (1987), Ourisson and Rohmer (1992), and R. Summons (pers. comm.)
22,29,30 tris-*nor*hopan-21-one (HOP)	Enriched in very degraded organic material in the water column, suggesting it is a refractory end product of bacteriohopanepolyol degradation	Conte et al. (1998a, b) and Konstadinos et al. (2001)
C_{10-18} β and $\omega-1$ hydroxy acids (HYDROXY ACIDS)	Gram-negative bacteria, including methanotrophs. $\omega-1$ acids also may be produced from aerobic hydroxylation of alkanes and acids	Jantzen and Bryn (1985), Skerratt et al. (1992), Goosens et al. (1986), and DeLeeuw et al. (1995)

highly degraded organic material may be dominated by only a few compounds such as cholesterol, the hopanone 22,29,30 tris-*nor*hopan-21-one and saturated fatty acids (Conte et al., 1998a; Kiriakoulakis et al., 2001).

The unsaturation ratio of the prymnesiophyte-derived C_{37} alkenones ($U^{K'}_{37}$) is defined as

$$U^{K'}_{37} = \frac{37{:}2}{37{:}2 + 37{:}3} \quad (1)$$

where 37:2 and 37:3 are the concentrations of the di- and tri-unsaturated C_{37} methyl alkenones. $U^{K'}_{37}$ is strongly correlated with the algae's growth temperature (Marlowe, 1984; Prahl et al., 1988; Conte et al., 1998b; Bijma et al., 2001). Conte et al. (2001b) have recently published a temperature calibration of $U^{K'}_{37}$ for the Bermuda time-series site based upon 7 years of surface water data:

$$T = 25.814 - 30.972(U^{K'}_{37}) + 33.694(U^{K'}_{37})^2 \quad (r^2 = 0.95, n = 91). \quad (2)$$

In sediment trap material, the $U^{K'}_{37}$ of alkenones will record the concentration-weighted mean of water temperatures at the time of alkenone synthesis, or an "integrated production temperature" (IPT, Conte et al., 1992). In the Bermuda region, alkenones are synthesized mainly within the upper euphotic zone (Haidar and Thierstein, 2001; Conte et al., 2001b). Therefore, the alkenone IPT of trap material primarily reflects surface water temperature. By comparison of alkenone IPT with surface temperature records, the mean date of alkenone synthesis and, in turn, the average net sinking velocity of alkenone-containing detritus can be estimated (cf. Conte et al., 1998a).

3. Sampling and analytical methods

3.1. The Oceanic Flux Program

The OFP mooring configuration is described in Conte et al. (2001a). The OFP traps (500, 1500, 3200 m depths) are McLane Parflux traps and have a 0.5 m^2 sampling area. Trap cups are filled with 40 ppt deep seawater (concentrated by freezing) and poisoned with ultra-trace metal purity $HgCl_2$ (200 mg l^{-1}). Only the 3200 m trap was in place for the time interval discussed here.

Methods for mass flux, bulk carbonate and organic carbon and nitrogen determination are described in Conte et al. (2001a). Briefly, 30% of the <1 mm size fraction of trap material is removed for lipid analysis and the remaining material is size-fractionated into 500–1000, 125–500 and <125 μm fractions and freeze dried. Mass flux is calculated from combined weights. Bulk analyses are made on the <125 μm size fraction, which constitutes $79+8$% of the total, and converted to total fluxes by assuming that the composition of the larger size fractions is similar.

Organic carbon was analyzed on a Perkin-Elmer 240B CHN instrument after decalcification of the sample by sulfurous acid treatment. Carbonate was measured on a Coulometrics coulometer. Total silicate, a residual fraction that includes both opal and lithogenic silicate, was estimated by difference according to the equation of Deuser et al. (1995):

$$\text{Total silicate} = \text{Mass} - \text{CaCO}_3 - (2.3 \times \text{Org C}). \quad (3)$$

Methods for lipid analyses are described in Conte et al. (1998a). Briefly, lipids were ultrasonically extracted with 2:1 chloroform:methanol. The lipid extract was transesterified with 5% methanolic HCl. The products were extracted into hexane and trimethylsilylated with BSTFA in pyridine. The transesterified, trimethylsilyl derivatives were gas chromatographed on a 60 m × 0.25 mm CPSil5CB column (0.25 μm film phase, Chrompack, USA) in a Fisons gas chromatograph with H_2 as the carrier gas. Compounds were identified by gas chromatograph–mass spectrometry (GC–MS) using an Autospec *Q* mass spectrometer under similar GC conditions except that He was used as the carrier gas. Selected samples were fractionated by Solid Phase Extraction to check for co-elution and to purify fractions for GC–MS. $U^{K'}_{37}$ was calculated from Eq. (1); analytical error was approximately 0.01 units. Alkenone IPT was estimated using Eq. (2).

A Lability Index (LI) was constructed to reduce the multi-dimensional biomarker information into a single, quantitative measure of changes in organic matter lability. An "LI" was calculated from Z standardized data on the relative abundance (as percent total extractable lipids (TELs) or total fatty acids) of selected diagnostic lipid biomarkers (Table 1):

$$\text{LI} = \sum(\text{PUFA} + \text{PS} + \text{LCK} + \text{DKA} + \text{ACG} + \text{SK} + \text{HOP}), \quad (4)$$

where PUFA = Σ(18:4ω3 + 18:5ω3 + 20:5ω3 + 22:6ω3); PS = Σ(C_{27} to $C_{29}\Delta^5$ and $\Delta^{5,22}$ + 4-methyl C_{30} sterols but excluding $C_{28}\Delta^5$); LCK = $C_{37–39}$ alkenones + C_{36} alkenoates; DKA = $C_{28–32}$ diols and ketols; ACG = 1–0 acylglycerols; SK = steroidal ketones; and HOP = $C_{30–33}$ hopanoic acids, alcohols and ketones.

3.2. The Bermuda Testbed Mooring

The present study focuses on the period from October 6, 1996 (day 280) to January 15, 1997 (day 381) during BTM Deployment #6. Zedler et al. (1997) and Dickey et al. (2001) provide details of the mooring configuration, instrumentation and functionality, sampling frequencies, calibrations, and data quality for this deployment. The mooring included temperature sensors at 2, 22, 34, 44, 54, 73, 76, 105, and 154 m, conductivity sensors at 44 and 73 m, and fluorometers at 20, 44 and 73 m. Only the raw fluorescence data are presented here as concurrent ship-based chlorophyll measurements were not sufficient to adequately calibrate the fluorescence in terms of chlorophyll *a* concentration. No direct meteorological data were available for the period of interest as the meteorological instrumentation failed after day 320. Therefore, NCEP reanalysis data were used to estimate meteorological parameters, as described in Dickey et al. (2001).

An RDI 150 kHz acoustic Doppler current profiler ADCP located at a depth of ~209 m provided horizontal currents and acoustic backscatter intensity from depths of about 22–202 m with 3 m vertical bin intervals (7.5 min averages). We used the ADCP data to estimate integrated 0–200 m zooplankton biomass by regressing ADCP backscatter intensity with zooplankton net tow data (L. Madin, unpublished data), as described in Jiang et al., (submitted).

3.3. The Bermuda Atlantic Time Series and ancillary measurements

BATS shipboard measurements and remote sensing studies provide additional information on the surface water environment. BATS sampling and analytical methods are reviewed in Steinberg et al. (2001). Temperature, salinity and chlorophyll fluorescence profiles were obtained from CTD casts made during BATS and OFP cruises. Pigment and nutrient analyses were made on selected CTD casts on each BATS cruise. Export

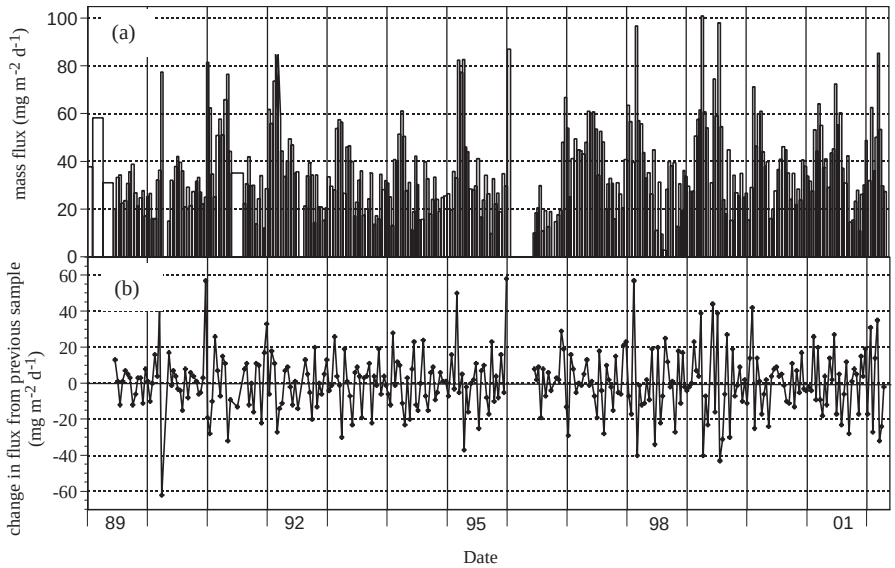

Fig. 1. (a) Biweekly integrated mass fluxes at 3200 m depth at the OFP site, 1989 to present. Each sample integrated flux over an approximate 2-week period and (b) change in mass flux from previous sample.

flux was obtained from 3-day deployments of a drifting sediment trap located at 200 m depth. Zooplankton biomass in the upper 200 m was determined from vertical net tows using a 200 μm mesh, 1 m^2 net (Madin et al., 2001).

Hindcast modeling of TOPEX and ERS data (McGillicuddy and Kosnyrev, 2001) provided information on sea-surface height anomalies and eddies during the study period. Animations generated from the objective analyses are available at http://science.whoi.edu/users/mcgillic/tpd/anim.html. It is worth noting that not all eddies are observable from satellite altimetry data and important subsurface structure (e.g., second baroclinic and higher mode eddies) cannot be inferred (e.g., McNeil et al., 1999; Dickey et al., 2001).

4. Results

4.1. Episodic high mass flux events in the 3200 m OFP record and the December 1996 flux event

Seasonal and non-seasonal variability in mass flux for the OFP record up to 1998 has been previously described in Conte et al. (2001a). The focus here is on the episodic occurrence of short-lived, abrupt increases in mass flux throughout the biweekly resolved deep flux record (Fig. 1a). Of the 293 mass flux data at 3200 m, 18.8% show an increase in mass flux of $>50\%$ from the previous sample. In contrast, only 7.5% of the samples show a decrease in flux of $>50\%$. Fig. 1b plots the change in mass flux from sample to sample. Ten percent of the samples (29) exhibit abrupt flux increases of $>20\,mg\,m^{-2}\,d^{-1}$ (for comparison, the average 3200 m mass flux is $37\,mg\,m^{-2}\,d^{-1}$). Abrupt flux increases occur most frequently in December–March with a secondary peak in June. In contrast, abrupt decreases in mass flux are more frequent in April and May.

Previously, Conte et al. (1998a) showed that the composition of trap material collected during an episodic high flux event in January 1996 was greatly enriched in labile organic material. Diagnostic biomarker compounds suggested that this event was associated with a phytoplankton bloom that was inefficiently remineralized in the upper ocean and was rapidly transported to depth. However, no upper ocean measurements were available for this time period to confirm these indications.

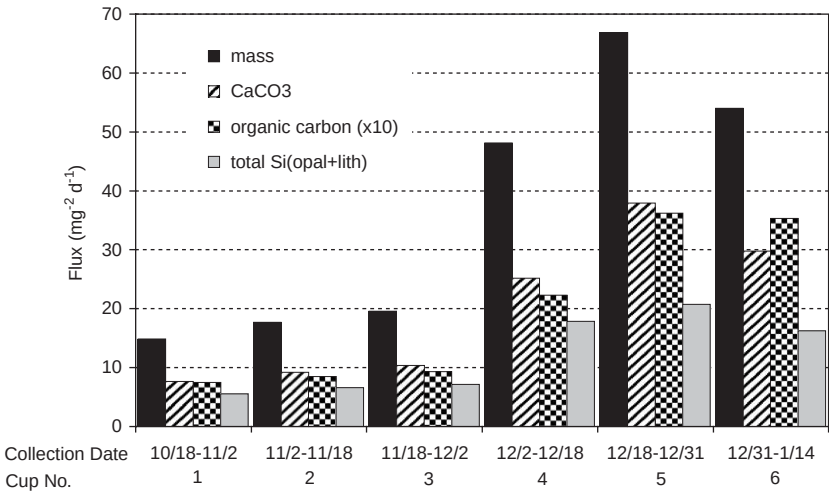

Fig. 2. Total mass flux at 3200 m depth and the fluxes of bulk components (organic carbon, calcite and total silicate) form the time period from October 18, 1996 (day of year 292) to January 14, 1997 (day of year 380). Total silicate is the residual after subtracting the carbonate and organic carbon from the mass, as described in the text, and includes both biogenic opal and lithogenic material.

In December 1996, another smaller abrupt increase in 3200 m mass flux was observed (Figs. 1a and b). Throughout this period, the BTM mooring was deployed and upper ocean conditions were also sampled during BATS and OFP cruises. The remainder of this paper focuses on the surface water forcing that precipitated the December 1996 flux event and how this short-lived event affected the export of labile, bioreactive material to the deep ocean.

The change in mass flux and the flux of the bulk components in the 3200 m trap between October 1996 and January 1997 is shown in Fig. 2. Between Cup 3 (collecting from 11/18 to 12/2) and Cup 4 (collecting from 12/2 to 12/18), the mass flux abruptly increased from 19 mg m^{-2} d^{-1} to almost 50 mg m^{-2} d^{-1}, an increase of 150%. Mass flux continued to increase by another 40% in Cup 5 (collecting from 12/18 to 12/31) before decreasing by about 25% in Cup 6 (collecting from 12/31 to 1/14). Abrupt flux increases were observed in all bulk flux components, but there were significant differences in their flux patterns. While carbonate and organic carbon fluxes continued to increase by 51% and 61%, respectively, between Cup 4 and Cup 5, silicate flux increased only by 16%. Between Cup 5 and Cup 6, both carbonate and residual silicate fluxes decreased by 28%, but organic carbon flux remained nearly constant.

4.2. Physical and biological structure of the overlying surface waters

BTM Deployment #6 (August 21, 1996–January 22, 1997, or day of year 234–388) began during the end of the summer stratification and extended through the period of surface layer cooling and mixed layer deepening (Fig. 3, also see Figs. 2 and 3 in Dickey et al., 2001). The physical conditions (see Fig. 3) for the period of focus, October 6, 1996–January 4, 1997, were characterized by: (1) relatively high wind stress (based on NCEP wind analyses described in Dickey et al., 2001); (2) monotonic cooling of near-surface waters; (3) highly variable temperature at depths of 7–154 m with major warming (by $\sim$4°C) first near the surface and about a month later at 154 m; (4) deepening of the mixed layer from about 50 to $>$154 m; (5) directional changes in currents (i.e., from generally southward day 310 to 330 to northward from day 338 to 341 to southward from day 350 to 370); and (6) currents with magnitudes of up to $\sim$50 cm s^{-1}. The most interesting aspect of the deployment involved the passage of a warm, low salinity apparently mesoscale feature with elevated biomass beginning in late November 1996 ($\sim$day 330). This feature was characterized by a thick, isothermal layer of at

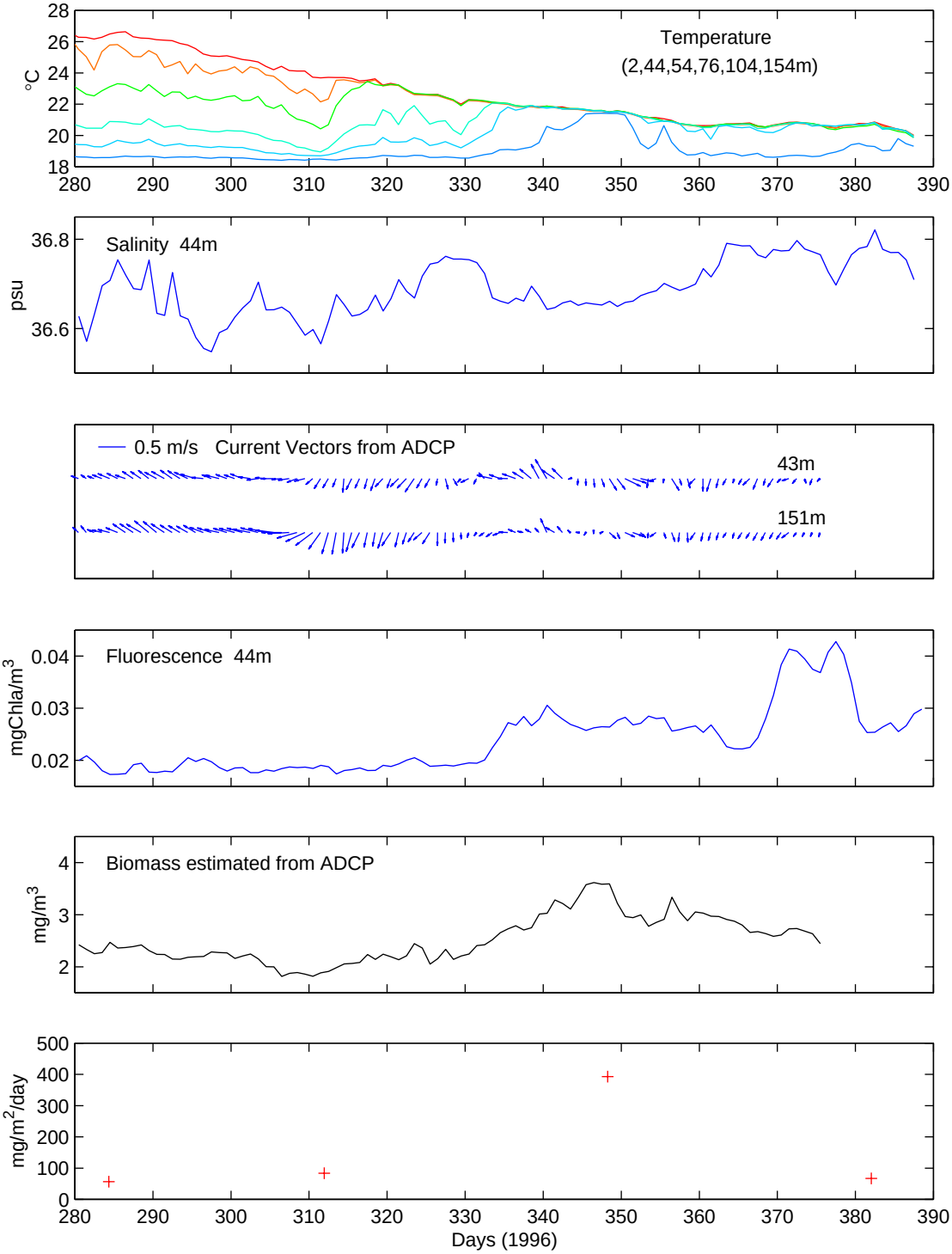

Fig. 3. Top four panels: continuous records of temperature, salinity currents, fluorescence and estimated zooplankton biomass measured at the BTM site from day of year 280 (October 6, 1996) to day 390 (January 24, 1997). Bottom panel: mass fluxes measured at 200 m depth from 3-day drifting trap deployments made on monthly BATS cruises.

least 180 m and clockwise rotational currents. Within the feature, sensors on the BTM mooring recorded roughly two-fold increases in chlorophyll fluorescence and in 0–200 m zooplankton biomass, as estimated from the ADCP data (Fig. 3). CTD data collected on BATS and OFP cruises (see below) provided supporting data which indicated that a mesoscale feature characterized by a thick warm, low salinity isostad passed through the time-series site in November and December.

CTD data collected during BATS and OFP cruises provided further information on the mixed layer and thermal structure and chlorophyll fluorescence within and outside (or away from) the feature (Fig. 4). The locations and dates of these casts (Fig. 5) suggest that the time-series site may have been on the extreme edge of the feature in mid-December as it passed through the area. CTD profiles of temperature, salinity and fluorescence taken on December 13 and 14 (day 348–349) show that the feature was characterized by a uniform high temperature and low salinity layer extending down to >180 m (Fig. 4). In contrast, the CTD profile taken on December 19 (day 354) showed the mixed layer to be only 100 m deep, which is typical of the average depth of the mixed layer in December (Steinberg et al., 2001), and was similar to the mixed layer depth measured in January 1997 on the subsequent BATS cruise.

TOPEX/ERS altimetry data (not shown) indicated that the southern edge of a warm eddy with inferred anticyclonic rotation (assuming first baroclinic mode) advected southwestward past the mooring early in November. This was consistent with the BTM current data. However, the warm, low salinity feature that influenced the site

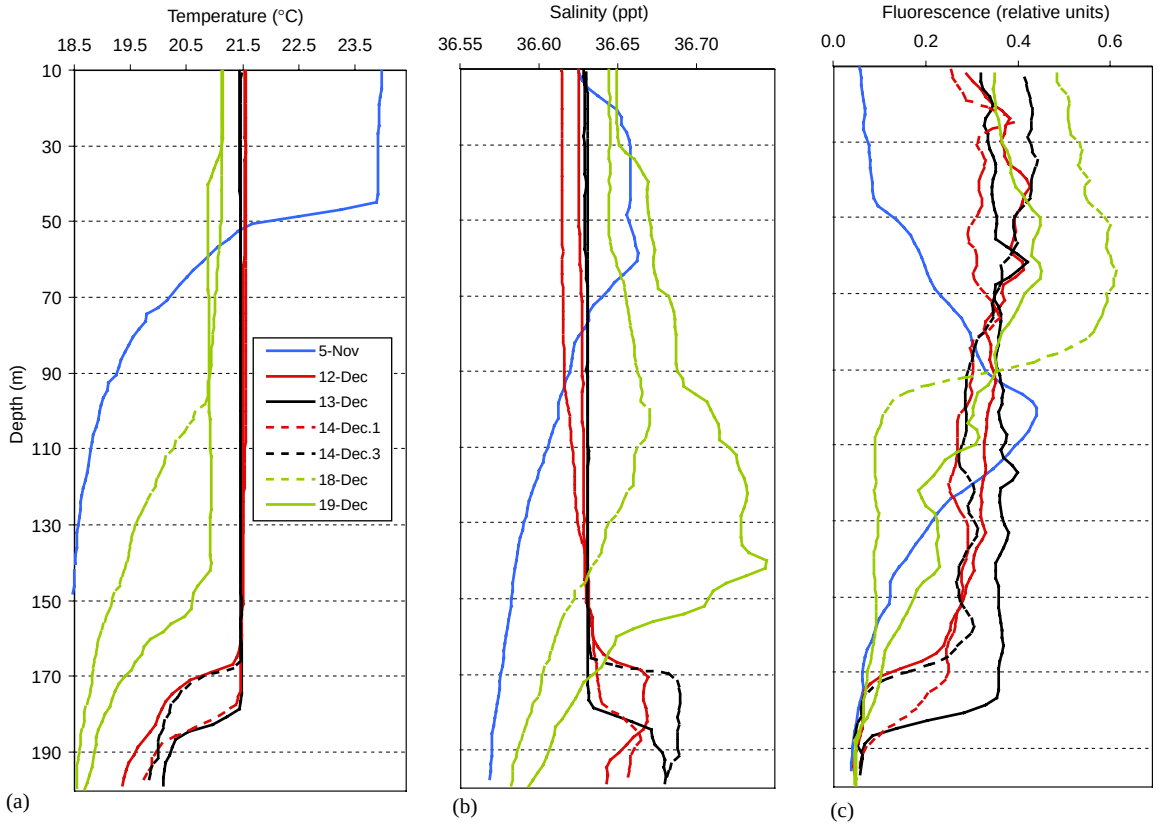

Fig. 4. CTD profiles of temperature (a), salinity (b) and fluorescence (c) measured on BATS and OFP cruises in December 1996. The locations of the casts are shown in Fig. 5. Profiles from a CTD cast collected on November 5 which shows the typical deep fluorescence maximum observed during the seasonal stratification period is given for comparison.

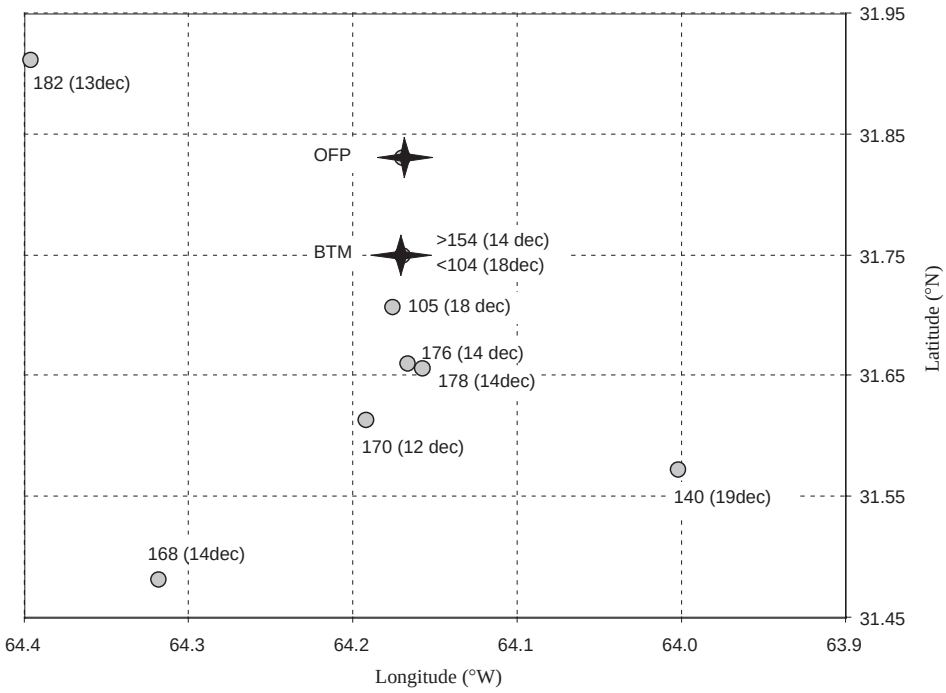

Fig. 5. Locations of CTD casts in December 1996 and the measured depth of surface isothermal layer. The date is given in parentheses. The locations of the OFP and BTM moorings are starred.

later in November and into December was not detected by satellite altimetry (see animated results from hindcast modeling of McGillicuddy and Kospyrev, http://science.whoi.edu/users/mcgillic/tpd/anim.html).

The mixed layer, which overlaid this mesoscale feature, appeared to be strongly forced, resulting in an increase in phytoplankton biomass, perhaps a bloom event. Dickey et al. (2001) used a turbulence closure mixed layer model to simulate the mixed layer deepening event. The model had no biological productivity component (chlorophyll was treated as a passive scalar). The modeled and observed mixed layer deepening were in good agreement with the chlorophyll mixing to form a uniform layer. However, the modeled depth integrated chlorophyll was less than that observed from BATS profile data. Dickey et al. (2001) suggest that the entrainment of nutrients into the euphotic layer may have been sufficient to induce a fall bloom. Horizontal advection associated with the mesoscale feature, which was not included in their model analyses because of lack of relevant horizontal data, may also have played a role.

Chlorophyll fluorescence profiles taken on December 13 and 14 (day 348–349) were also uniform with depth to >180 m, and indicated deep mixing of phytoplankton biomass to nearly twice the euphotic zone depth (Fig. 4c). CTD bottle data for phytoplankton pigments from this cast similarly showed uniform pigment and TCO_2 concentrations and uniform POC/PON ratios down to the base of the thermostad (Steinberg et al., 2001), consistent with active deep mixing. However, several other casts taken within the feature exhibited slight gradients in chlorophyll fluorescence. This indicated that deep mixing was not continuously active with respect to phytoplankton growth over the entire period. This suggested transient mixed layer stabilization, possibly as a result of variations in atmospheric forcing, or slight spatial heterogeneity across the feature.

BATS nutrient profiles (Steinberg et al., 2001) provided clear evidence for nutrient entrainment

into the euphotic zone by deep mixing, and support the conclusions of Dickey et al. (2001) based upon modeling results. The nutricline in January 1997 (day 381 and day 395), after the feature had passed, was located at a depth of about 90–100 m at the base of the mixed layer. In contrast, nitrate concentrations within the feature were about 0.8 μmol kg^{-1} and invariant in concentration from the surface to depths > 160 m (see November 6 cast, day 311), clearly indicative of active mixing of nutrients into the euphotic zone.

In spite of evidence for enhanced nutrient supply, the water column integrated phytoplankton biomass at the time of sampling was not substantially higher within the feature than in surrounding waters. The integrated 0–200 m chlorophyll fluorescence (in relative units) ranged from 68 units in the December 14 (day 349) cast taken nearest the apparent center of the mesoscale feature to 55 units in the December 20 (day 355) cast taken near the periphery. The integrated 0–200 m chlorophyll fluorescence in the December 19 (day 354) cast taken at the edge of the feature was 60 units, similar to that observed within the feature, although this chlorophyll fluorescence was shallower and concentrated within the 95 m thick mixed layer.

Phytoplankton community structure in the feature, as assessed from measurements of HPLC pigments on December 12 (day 347), was significantly distinct from that measured in November 1996 or later in January (Fig. 6). Pigment profiles also clearly indicated deep mixing of phytoplankton cells within the feature's thermostad. Concentrations of chlorophyll $c1 + c2$, fucoxanthin and prasinoxanthin were of 2–4 times higher in the feature than in January after the feature had passed. This suggested that diatom and prasinophyte production in particular was stimulated by the physical and nutrient environment within the feature, even though low concentrations of these pigments indicated that these taxa remained minor phytoplankton biomass components. Concentrations of 19′-butanoyloxyfucoxanthin, 19′-hexanoyloxyfucoxanthin and diadinoxanthin were also greatly elevated in the feature and indicated significantly higher standing stocks of prymnesiophytes, pelagophytes and other taxa containing these pigments. Surface concentrations of these pigments decreased after the feature had passed (see cast on January 14, day 380) but then increased in a later cast taken on January 28 (day 394). In contrast to these pigments, concentrations of zeaxanthin + lutein, cyanobacteria indicators, and chlorophyll *b*, a prochlorophyte indicator, were not significantly higher in the feature, although zeaxanthin + lutein concentrations increased later in January. This suggested that the conditions in the feature did not stimulate cyanobacteria and prochlorophyte production as strongly as other groups. Concentrations of peridinin, a dinoflagellate indicator, also were not significantly higher in the feature and indicated that dinoflagellates were very minor components of the phytoplankton biomass. This is consistent with the long-term BATS record (Steinberg et al., 2001) and also with the very low surface water concentrations of dinosterol, a dinoflagellate sterol (M. Conte, unpublished data). These results are similar to those of Sweeney et al. (in press), who observed elevated concentrations of diatom and prymnesiophyte pigments but not cyanobacteria, prochlorophyte or dinoflagellate pigments in mode water and cyclonic eddies that contained high chl *a* concentrations.

Zooplankton biomass and 200 m export flux also significantly increased when the feature arrived at the time-series site (Fig. 3). ADCP estimates of 0–200 m zooplankton biomass increased by roughly 50% when the feature arrived at the BTM site and peaked on December 13–14 when the central portion of the feature appeared to be directly over the mooring (Figs. 3 and 4). This was confirmed by zooplankton net tow data (Madin et al., 2001). Within the feature, zooplankton biomass in the upper 200 m averaged 785 mg m^{-2} at midday and 1082 mg m^{-2} at night (Madin et al., 2001). This was more than double the zooplankton biomass observed in either November 1996 or January 1997 and the highest December zooplankton biomass measured over a 5-year period (Madin et al., 2001).

The higher zooplankton biomass within the feature suggests that phytoplankton standing stock relative to production may have been depressed by higher grazing pressure. This is

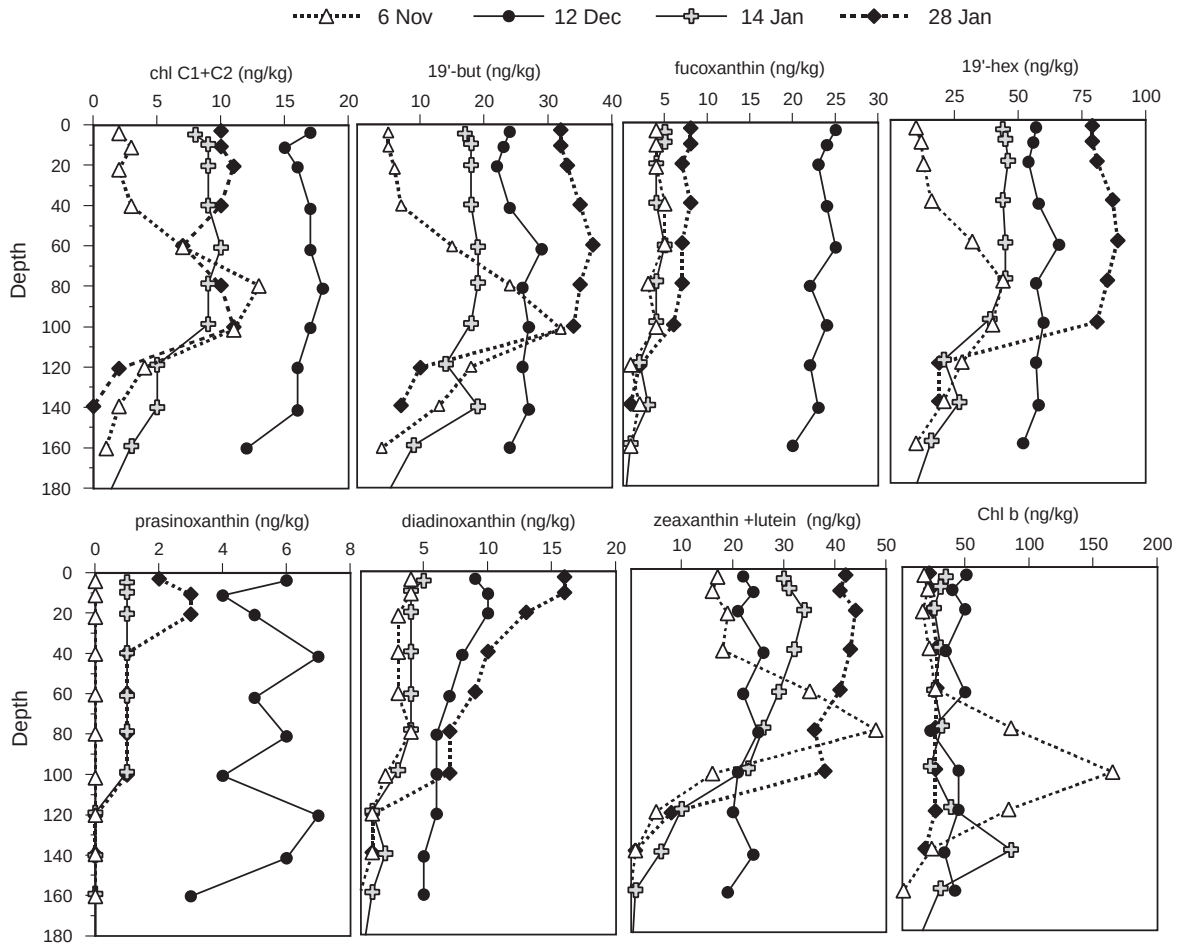

Fig. 6. Pigment profiles collected on BATS cruises on days of year 311 (November 6), 347 (December 12, within the feature, cf. Fig. 4), 380 (January 14, 1997) and 394 (January 28, 1997). 19′-but and 19′-hex represent 19'-butanoyloxyfucoxanthin and 19′-hexanoyloxyfucoxanthin, respectively.

supported by the extremely high mass fluxes measured by the drifting trap deployed just below the feature's thermostad (Fig. 3). The 200 m export flux was nearly 400 mg $m^{-2} d^{-1}$ for this deployment, or ~32 mg C $m^{-2} d^{-1}$. This was more than a factor of 5–6 higher than the mass flux and a factor of 2 higher than the carbon flux in November 1996 or in January 1997 after the feature had passed.

Vertically migrating zooplankton were likely to also contribute to export flux (cf. Dam et al., 1995; Zhang and Dam, 1997; Steinberg et al., 2000; Al-Mutari and Landry, 2001). Vertically migrating zooplankton carbon, calculated from the day–night 0–200 m biomass data and a carbon to dry weight conversion of 0.37 (Madin et al., 2001), was ~110 mg C m^{-2}. Using zooplankton CO_2 respiration + DOC excretion rates given in Steinberg et al. (2000) (0.04–0.08 mg C mg^{-1} body C d^{-1}), migratory CO_2 + DOC flux was estimated as 4.4–8.8 mg C m^{-2}, or about 11–20% of the 200 m trap carbon flux. Zooplankton mortality at depth, roughly estimated to be about 30–70% of the DIC flux (Al-Mutari and Landry, 2001), would result in an additional 1.3–6 mg C $m^{-2} d^{-1}$ of migratory zooplankton carbon exported to the midwater ecosystem.

The coincidence of the presence of this productive feature at the site in late November to mid-December strongly suggests that the abrupt increase in deep flux observed in the OFP trap (Fig. 2) was directly linked to the passage of this feature across the trap's surface catchment area (cf. Siegel and Armstrong, 2002). However, bulk flux data provide no concrete evidence to confirm this conclusion. In the following section, we use the diagnostic lipid biomarkers that are present in the recovered trap material to directly link the passage of this feature with the deep flux event and also to assess its effect on deep flux composition. These data also provide new evidence for the mediating role of midwater zooplankton in coupling surface processes with deep ocean flux.

4.3. Compositional changes in 3200 m trap material

Concentrations of bulk flux components and of major lipid classes and selected diagnostic biomarkers in the 3200 m trap material are given in Table 2a. Bulk composition did not change substantially when mass flux first increased (Cup 4, December 2–18). However, the percentage of organic carbon and carbonate increased 17% and 8%, respectively, while residual silicate decreased 17% in the subsequent collection period (Cup 5, December 18–31).

Larger variations in the concentrations of TELs and individual lipid biomarkers were also observed over this period. As seen in bulk composition, lipid composition showed the largest change in Cup 5 (December 18–31), after the abrupt increase in mass flux. The total concentration of extractable lipids, which make up about 1–1.5% of organic carbon, increased 63% from Cup 4 (December 2–18) to Cup 5 (December 18–31) and remained elevated in Cup 6 (December 31–January 14).

For individual lipid biomarkers, the magnitude of the concentration increase reflected their different sources and lability. Primary phytoplankton-derived compounds such as phytosterols, alkenones and alkyl alkenoates, diols and ketols doubled or tripled in concentration in Cup 5 (December 18–31) and remained elevated. Steroidal ketones and stanols, early sterol degradation products and the bacteria-derived β and $\omega-1$ hydroxy acids and hopanoids also doubled or tripled in concentration in Cup 5. In comparison, concentrations of cholesterol and saturated and monounsaturated fatty acids, including the bacteria-derived odd and branched chained acids, did not change substantially over the analysis period. Concentrations of the zooplankton biomarker 18:1ω9 and the hopanone 22,29,30 tris-*nor*hopan-21-one, a presumed end product of bacteriohopanepolyol degradation, decreased when the mass flux abruptly increased (Cup 4, December 2–18) and remained low throughout the rest of the analysis period. Their concentration decrease suggested that the detrital material(s) containing these compounds was diluted by addition of fresh, labile phytoplankton-derived material. The temporal change in PUFA concentrations (18:4ω3, 18:5ω3, 20:5ω3 and 22:6ω3) differed from both phytoplankton-derived biomarkers and early degradation products and abruptly increased in Cup 3 (November 18–December 2), before the mass flux increase.

To reduce the multi-dimensional lipid biomarker information to a single quantitative indicator of organic matter composition, we calculated a simple "LI" (Eq. (4)) using the relative abundances of key diagnostic biomarkers. The LI index successfully captured the major changes observed in lipid biomarker composition. LI increased systematically from -8.2 in cup 1 to 10.2 in cup 5 with the largest change observed between Cup 4 and Cup 5, consistent with the rapid increases in concentrations of phytoplankton and microbial biomarkers.

In summary, the biomarker data show that relative contribution of fresh, labile phytoplankton-derived organic material in the trap cups began to increase in Cup 3 (November 18–December 2) when the mesoscale feature was first observed at the BTM site. The concentration of labile material then rapidly increased in Cup 4 (December 2–18) and peaked in Cup 5 (December 18–31). The timing of this change in organic matter composition and its lability provides strong evidence to link the pulse in deep flux with the passage of the productive mesoscale feature through the area. The strong covariance between concentrations of phytoplankton-derived

Table 2
Concentrations of bulk constituents (percentage of dry weight) and of diagnostic lipid biomarkers in the 3200 m trap material ($\mu g\,gdw^{-1}$) (October 1996–January 1997), relative abundances (as percentage of total extractable lipids or fatty acids) of major biomarker classes in the trap material, and lability index of organic material (LI) in the trap cups

Cup no.	1	2	3	4	5	6
Start date	18-Oct-96	2-Nov-96	18-Nov-96	2-Dec-96	18-Dec-96	31-Dec-96
End date	2-Nov-96	18-Nov-96	2-Dec-96	18-Dec-96	31-Dec-96	14-Jan-97
Days open	15	16	14	14	13	14
(a) Concentrations						
Bulk constituents (% of dry weight)						
$CaCO_3$	51.3	51.9	52.8	52.3	56.6	55.0
Organic carbon	5.0	4.8	4.7	4.6	5.4	6.5
Total "silicate"[a]	37.2	37.0	36.3	37.1	30.9	30.0
Lipid biomarker concentrations ($\mu g\,gdw^{-2}$)						
Total extractable lipids (TEL)	758	534	631	552	902	757
Total fatty acids (TFA)	190.0	103.8	156.0	124.9	150.5	156.6
Saturated $\leqslant C_{24}$ acids (SAT)	52.0	17.5	25.4	22.4	30.8	25.7
Monounsaturated $\leqslant C_{24}$ acids (MONO)	42.6	34.2	47.8	34.8	47.0	48.0
18:1ω9	22.2	18.3	25.1	14.9	13.5	16.4
Polyunsaturated fatty acids (PUFAs)	25.0	17.6	33.4	25.5	33.3	33.5
18:5ω3	0.24	0.15	0.76	0.44	0.74	0.69
18:4ω3	0.49	0.50	1.20	1.01	1.69	1.77
20:4ω6	2.02	0.94	2.36	1.69	1.73	1.30
20:5ω3	4.77	2.46	4.61	5.20	5.53	4.50
22:6ω3	3.41	6.83	14.86	10.51	14.64	15.10
20:5ω3/22:6ω3 ratio	1.40	0.36	0.31	0.49	0.37	0.30
Odd + branched acids (ODD/BR)	10.17	6.53	8.54	11.06	7.77	12.16
$\beta+\omega-1$ hydroxy acids	1.98	1.62	1.57	1.65	2.86	2.22
Total sterols + stanols	90.69	100.07	105.86	112.72	220.89	153.65
Phytosterols[b]	40.14	43.46	55.69	55.32	119.22	87.96
Choles-5-en-3β-ol (cholesterol)	40.82	45.85	37.42	41.21	51.63	40.02
Stanols	9.73	10.75	12.75	16.18	50.05	25.68
Steroidal ketones	4.25	4.93	7.77	9.38	36.56	13.62
Alkenones + alkyl alkenoates (LCK)	5.08	7.10	6.93	21.45	66.33	29.35
C_{28-30} alkan-1,15-diols + alkan-15-one-1-ols	23.31	24.19	25.75	23.79	55.28	55.20
Other diols[c]	8.35	11.88	16.39	16.64	41.38	31.75
1-0-Alkylglycerols	0.21	0.06	0.17	0.29	1.04	0.50
C_{30-32} hopanols + hopanoic acids (HOPANOIDS)	14.90	14.61	15.40	14.12	40.94	23.82
22,29,30 tris-*nor*hopan-21-one (HOP)	66.06	66.52	61.44	49.61	45.37	30.91
(b) Relative abundances						
Total extractable lipids (TEL) (% Org C)	1.5	1.1	1.3	1.2	1.7	1.2
Phytosterols (% TEL)	5.3	8.1	8.8	10.0	13.2	11.6
LCK + AA (% TEL)	0.7	1.3	1.1	3.9	7.4	3.9
PUFAs (4–6 bonds) (% TFA)	6.6	11.9	16.7	16.6	17.2	16.8
ODD/BR (% TFA)	5.3	6.3	5.5	8.8	5.2	7.8
DIOLS/KETOLS[d] (% TEL)	4.2	6.8	6.7	7.3	10.7	11.5
1-O-Acylglycerols(% TEL)	0.0	0.0	0.0	0.1	0.1	0.1
$>C_{27}$ HOPANOIDS (% TEL)	2.0	2.7	2.4	2.6	4.5	3.1
Steroidal ketones (% TEL)	0.6	0.9	1.2	1.7	4.1	1.8
(*c*) Lability index[e] (LI)	−8.2	−4.0	−2.4	0.5	10.2	3.8

Note: The shorthand notation of lipid classes is given in parentheses.
[a] Total "silicate" = Mass − $CaCO_3$ − (2.3 × Org C) and includes opal + lithogenic Si.
[b] PS = sum of $C_{27-29}\Delta^5$ and $\Delta^{5,22}$ sterols (excluding cholesterol) + 4α,23,24-trimethyl-5α-choles-22-en-3β-ol (dinosterol).
[c] Principally C_{28} and C_{30} diols.
[d] Includes all C_{28-32} diols and ket-1-ols.
[e] Defined in Eq. (4).

biomarkers, early lipid degradation products and bacteria-derived biomarkers suggests that the settling phytoplankton detritus was actively being degraded as it entered the trap, consistent with the findings of Conte et al. (1998a) for the pulsed flux event in January 1996.

4.4. Flux patterns of lipid biomarkers

There was a dramatic effect of this mesoscale feature on lipid biomarker fluxes (Table 3). TEL flux increased by 30% in Cup 4 (December 2–18) and a further 127% in Cup 5 (December 18–31) and then declined by 30% in Cup 6 (December 31–January 14). The peak flux in Cup 5 was nearly five times that before the feature arrived (Cup 3, November 18–December 2).

The flux pulse of phytoplankton-derived biomarkers was more intense but of shorter duration than the flux pulse of the TELs. Fluxes of phytoplankton biomarkers increased 200–400% from Cup 4 to Cup 5, and then declined by 40–60% in Cup 6 (December 31–January 14). Peak fluxes of phytosterols, $C_{30–32}$ diol and ket-1-ol were seven times those observed in Cup 3. For alkenones, the peak flux was 30 times higher in

Table 3
Fluxes of bulk constituents and lipid biomarkers in the 3200 m OFP trap, October 96–January 97

Cup no.	1	2	3	4	5	6	Flux ratio
Start date	18-Oct-96	2-Nov-96	18-Nov-96	2-Dec-96	18-Dec-96	31-Dec-96	Cup 5:
End date	2-Nov-96	18-Nov-96	2-Dec-96	18-Dec-96	31-Dec-96	14-Jan-97	Cup 3
Days sampling	15	16	14	14	13	14	
Bulk constituent fluxes ($mg\,m^{-2}\,d^{-1}$)							
Mass	14.8	17.6	19.5	48.1	66.9	54.0	3.4
$CaCO_3$	7.60	9.15	10.31	25.14	37.87	29.71	3.7
Organic carbon	0.74	0.84	0.93	2.23	3.62	3.53	3.9
Total "silicate"	5.51	6.52	7.08	17.83	20.67	16.18	2.9
Lipid biomarker fluxes ($\mu g\,m^{-2}\,d^{-1}$):							
Total extractable lipids (TEL):	11.23	9.40	12.33	26.55	60.29	40.85	4.9
Total fatty acids (TFA)	2.81	1.83	3.05	6.00	10.07	8.46	3.3
Even saturated $\leqslant C_{24}$ acids (SAT)	0.77	0.31	0.50	1.08	2.06	1.39	4.1
Even monounsaturated $\leqslant C_{24}$ acids (MONO)	0.61	0.60	0.93	1.68	3.14	2.59	3.4
18:1ω9	0.33	0.32	0.49	0.72	0.91	0.89	1.9
Polyunsaturated fatty acids (PUFAs)	0.37	0.31	0.65	1.23	2.23	1.81	3.4
18:5ω3	0.004	0.003	0.015	0.021	0.049	0.037	3.3
18:4ω3	0.007	0.009	0.023	0.049	0.113	0.096	4.2
20:4ω6	0.030	0.017	0.046	0.081	0.115	0.070	2.5
20:5ω3	0.071	0.043	0.090	0.250	0.370	0.243	4.1
22:6ω3	0.050	0.120	0.290	0.505	0.979	0.815	3.4
Odd + branched acids	0.15	0.12	0.17	0.53	0.52	0.66	3.1
$\beta+\omega-1$ hydroxy acids	0.03	0.03	0.03	0.08	0.19	0.12	6.3
Total sterols + stanols	1.34	1.76	2.07	5.42	14.77	8.30	7.1
Phytosterols	0.60	0.77	1.09	2.66	7.97	4.75	7.3
Choles-5-en-3β-ol (cholesterol)	0.61	0.81	0.73	1.98	3.45	2.16	4.7
Stanols	0.14	0.19	0.25	0.78	3.35	1.39	13.4
Steroidal ketones	0.06	0.09	0.15	0.45	2.45	0.74	16.3
Alkenones + alkyl alkenoates (LCK + AA)	0.08	0.13	0.14	1.03	4.44	1.59	31.7
$C_{28–30}$ alkan-1,15-diols + alkan-15-one-1-ols	0.35	0.43	0.50	1.14	3.70	2.98	7.4
Other diols	0.12	0.21	0.32	0.80	2.77	1.72	8.7
1-0-Alkylglycerols	0.003	0.001	0.003	0.014	0.069	0.027	23.0
$C_{30–32}$ hopanols + hopanoic acids (HOPANOIDS)	0.22	0.26	0.30	0.68	2.74	1.29	9.1
22,29,30 tris-*nor*hopan-21-one (HOP)	0.98	1.17	1.20	2.39	3.03	1.67	2.5

Note: The shorthand notation for lipid classes is given in parentheses.

Cup 5 than in Cup 3! Peak fluxes of steroidal ketones, stanols, β and $\omega-1$ hydroxy acids, hopanoids and 1-O-acylglycerols were similarly 5–20 times higher in Cup 5 than in Cup 3.

Table 4 contrasts the fluxes of bulk components and specific biomarkers during the 6-week period before the passage of the mesoscale feature (Cups 1–3) with the following 6-week period when the mesoscale feature influenced the site (Cups 4–6), and contrasts these data with the 13-year (1989–2001) means for the two time periods. In October–December 1996, mass flux was 35% lower than the 13-year mean, whereas in December–January 1996/97 the mass flux was 60% higher than the long-term mean. There was a factor of two difference in mass flux between the two periods, significantly larger than the long-term average difference of 40%.

For extractable lipids, saturated and monounsaturated acids, and zooplankton-derived compounds

Table 4
Comparison of 6-week average 3200 m fluxes of bulk constituents and lipid biomarkers before arrival of mesoscale feature at the time-series site (Cups 1–3) with fluxes during the peak flux period (Cups 4–6)

Cup no.	Cups 1–3	Cups 4–6		Flux increase
Start date	18-Oct-96	2-Dec-96	% increase in flux	relative to Org C
End date	2-Dec-96	14-Jan-97		
Mass flux ($mg\,m^{-2}\,d^{-1}$)	15.8	56.3	256	0.87
Mass flux: 1989–2001 (mean $\pm$ s.d.)	24.3 ± 5.4	34.8 ± 14.8	43	
Bulk constituents ($mg\,m^{-2}\,d^{-1}$)				
$CaCO_3$	8.23	30.90	275	0.92
Organic carbon	0.77	3.13	306	—
Total "silicate"	5.80	18.23	214	0.77
Lipid biomarkers ($\mu g\,m^{-2}\,d^{-1}$)				
22,29,30 tris-*nor*hopan-21-one	1.02	2.36	131	0.57
18:1ω9 fatty acid	0.35	0.84	140	0.59
20:4ω6 fatty acid	0.03	0.09	200	0.77
Even saturated C_{12-24} acids (SAT)	0.48	1.51	215	0.77
Total fatty acids (TFA)	2.34	8.18	250	0.85
Even monounsaturated C_{12-24} acids	0.65	2.47	280	0.93
Choles-5-en-3β-ol (cholesterol)	0.65	2.53	289	0.94
Total extractable lipids (TEL)	10.00	42.57	326	1.04
Odd + branched acids	0.13	0.57	338	1.04
Polyunsaturated fatty acids (PUFAs)	0.40	1.76	340	1.06
20:5ω3 fatty acid	0.06	0.29	383	1.13
$\beta+\omega-1$ hydroxy acids	0.03	0.13	333	1.16
18:5ω3 fatty acid	0.01	0.04	300	1.30
22:6ω3 fatty acid	0.14	0.77	450	1.34
C_{30-33} hopanoids	0.24	1.57	554	1.62
C_{28-30} alkan-1,15-diols + alkan-15-one-1-ols	0.39	2.61	569	1.63
Phytosterols	0.75	5.13	584	1.67
18:4ω3 fatty acid	0.01	0.09	800	1.77
C_{28-30} diols	0.20	1.76	780	2.18
Stanols	0.18	1.84	922	2.55
Steroidal ketones	0.09	1.21	1244	3.25
1-0-Alkylglycerols	0.00	0.04	1112	4.20
Alkenones + alkyl alkenoates	0.11	2.35	2036	5.40

Note: The 13-year (1989–2001) average mass flux for these two time periods is shown for comparison. Details of lipid biomarker classifications are given in Table 2.

(e.g., cholesterol, 18:1ω9, 20:4ω6), the difference in fluxes between the two time periods was similar to that observed for organic carbon. However, much larger flux differences were observed for PUFAs, phytoplankton-derived biomarkers, and for bacteria-derived biomarkers. Flux differences between the two periods were especially pronounced for alkyl diols and stanols, steroidal ketones, 1-0-alkylglycerols and alkenones and were factors of 2–6 larger than the flux difference observed for organic carbon.

Consistent with inferences from concentration data, the timing of the very pronounced peak in fluxes of labile phytoplankton-derived biomarkers (and early degradation products) provides strong evidence that the 3200 m OFP trap intercepted phytoplankton-laden detritus that settled from this productive feature. The coincident increases in fluxes of several taxonomically distinctive biomarkers indicated that several phytoplankton groups contributed to this bloom/flux event. A particularly large contribution from the coccolithophore *E. huxleyi* is indicated by the extreme increase in alkenone flux, and accompanying increase in fluxes of 18:5ω3, 22:6ω3 and the $C_{28}\Delta^{5,22}$ sterol (data not shown), all of which are present in high concentrations in *E. huxleyi*. In contrast, diatoms did not appear to be major contributors to this event, as evidenced by the low 20:5ω3/22:6ω3 ratio and the very low fucoxanthin concentrations in the thermostad of the feature (Fig. 6).

4.5. The time lag between surface forcing and deep flux

We used the C_{37} alkenone unsaturation index ($U^{K'}_{37}$) of alkenones in the trap material and the Bermuda temperature calibration (Eq. (2)) to calculate the alkenone "IPT", or the concentration-weighted mean of the production temperatures, for alkenones in the trap cup. We then compared the alkenone IPT in the trap with BTM and BATS surface water temperature records to estimate the mean date of alkenone synthesis. To estimate the flux of alkenones from recent production ($Flux_{new}$), we assume that the increase in alkenone flux from that of the previous cup was caused by an increase in alkenone flux from recent surface water production:

$$Flux_{new} = Flux_t - Flux_{t-1}, \quad (5)$$

where flux is in $\mu g\, m^{-2}\, d^{-1}$ and the subscripts t and $t-1$ indicate consecutive times. For this first-order estimate, we assume that the $U^{K'}_{37}$ ratio of "baseline" flux of alkenones is similar to that measured in the previous trap cup. The $U^{K'}_{37}$ ratio of the flux of "new" alkenones can be then estimated as

$$U^{K'}_{37new} = \frac{(U^{K'}_{37t})(Flux_t) - (U^{K'}_{37t-1})(Flux_{t-1})}{Flux_{new}} \quad (6)$$

The IPT of recently synthesized alkenones in Cup 4 (December 2–18), the cup with the initial increase in alkenone flux, is estimated as 24.0°C. This IPT estimate corresponds to mixed layer temperatures in early November (Fig. 3). The IPT of alkenones collected in Cup 5 (December 18–31), the peak flux period, was 23.2°C. This IPT estimate corresponds to mixed layer temperatures in mid-November, when the mesoscale feature was well within the 3200 m trap's catchment area (cf. Siegel and Armstrong, 2002).

The approximate mean synthesis dates for alkenones collected in the deep trap, as indicated by the alkenone IPT, show that it took approximately 4–6 weeks for alkenone-containing detritus to settle from the surface to 3200 m depth. This translates into an average settling velocity of 75–115 $m\, d^{-1}$, consistent with other estimates of the settling velocities of phytoplankton detritus (e.g., Lampitt, 1985; Rice et al., 1986; Diercks and Asper, 1997; Conte et al., 1998a). As individual *E. huxleyi* cells are only 3–4 μm in size, this estimated sinking velocity provides clear evidence for intense biological aggregation in surface waters. This conclusion is also supported by the very high zooplankton biomass within the feature (Fig. 3 and Madin et al., 2001) and also by the very high mass flux measured just below the feature's thermostad (Fig. 3).

Although surface water temperature decreased between October and December (Fig. 3), the alkenone IPT in Cups 1–3 increased. Similar results were observed in November 1995–January 1996 (Conte et al., 1998a). This observation is counter to expectations if the alkenone flux was

Table 5
Alkenone and alkyl alkenoate flux at 3200 m and the C_{37} alkenone unsaturation ratio ($U^{K'}_{37}$) in the trap material

Collection dates	10/18–11/2	11/2–11/18	11/18–12/2	12/2–12/18	12/18–12/31	12/31–1/14
Cup no.	1	2	3	4	5	6
Alkenone + alkenoate flux ($\mu g\,m^{-2}\,d^{-1}$)	0.075	0.125	0.135	1.032	4.435	1.585
$U^{K'}_{37}$ of trap material	0.72	0.79	0.80	0.85	0.83	0.83
New production flux ($\mu g\,m^{-2}\,d^{-1}$)	—	0.050	0.010	0.896	3.403	—
Est. $U^{K'}_{37}$ of new production	0.72[a]	0.91	0.91	0.86	0.83	0.83
Est. IPT of new production	20.9[a]	25.4	25.5	24.0	23.2	23.4
Julian day when SST = IPT		293	294	310	322	320
Date when SST = IPT	~Late Apr	20-Oct	20-Oct	5-Nov	15-Nov	15-Nov

Note: The flux of recent alkenone production and its $U^{K'}_{37}$ index were estimated as described in the text. The alkenone integrated production temperature (IPT) was estimated using a non-linear temperature calibration of $U^{K'}_{37}$ derived for the Bermuda region (Eq. (2)). The approximate date when overlying surface mixed layer temperature (SST) equaled alkenone IPT was determined from BTM and BATS records.

[a] Alkenone $U^{K'}_{37}$ and IPT are calculated for the total alkenones in the trap cup.

derived solely from recent surface production. As shown in Table 4, alkenone IPT for the peak flux was consistent with recent synthesis in surface waters, but the IPT of the total alkenone flux during the low flux period (Cup 1, October 18–November 2) was only 20.9°C. This IPT estimate corresponds to surface temperatures in April (Steinberg et al., 2001). One explanation for the low IPT in Cup 1 is that during highly stratified summer conditions alkenone synthesis occurs mainly at the base of the seasonal thermocline at the depth of the deep chlorophyll maximum. However, both *E. huxleyi* cell profiles (Haidar and Thierstein, 2001) and alkenone concentrations (Conte et al., 2001b) at the time-series site indicate only minimal alkenone production at this depth. A second possibility is that a significant proportion of the deep-water alkenone flux during periods of low productivity is supported by repackaging of suspended alkenones into larger settling particles. Water column studies of alkenone distributions indicate that the inventory of alkenones in the suspended particle pool far exceeds that in the large particle pool (Conte et al., 1995), and that the alkenones in deep suspended matter have a temperature signal that reflects the season of maximum production and flux (Conte et al., 1992). Similarly, the alkenone IPT measured here during the low flux period (20.9°C) is skewed towards the surface mixed layer temperatures during the alkenone seasonal production maximum at Bermuda (estimated to be ~22°C, Conte et al., 2001b), supporting a "scavenged flux" component derived from biological repackaging of suspended materials (Table 5).

4.6. The temporal phasing of deep flux components

Histograms of the fluxes of mass, bulk components and lipid biomarkers, normalized to the peak flux, clearly indicate significant differences in temporal phasing for different flux components (Fig. 7). In particular, the abrupt flux pulse of phytoplankton and bacterial biomarkers clearly lags the initial increase in the fluxes of bulk components and is of shorter duration and more pronounced than for bulk components. Flux patterns of steroidal ketones, stanols, 1-0-acylglycerols and the bacteria-derived hydroxy acids and $C_{30–32}$ hopanoids were very similar to those of the phytoplankton biomarkers, and support the conclusion that these compounds were intimately associated with the labile, phytoplankton detritus. In contrast, flux patterns of TELs, and saturated, monounsaturated and PUFAs were more similar to those observed for bulk components.

The difference in temporal phasing of the PUFA flux is notable. These compounds are highly labile and have half-lives in detritus on the order of a few days (Conte, 1989). Thus, if the trap first collected

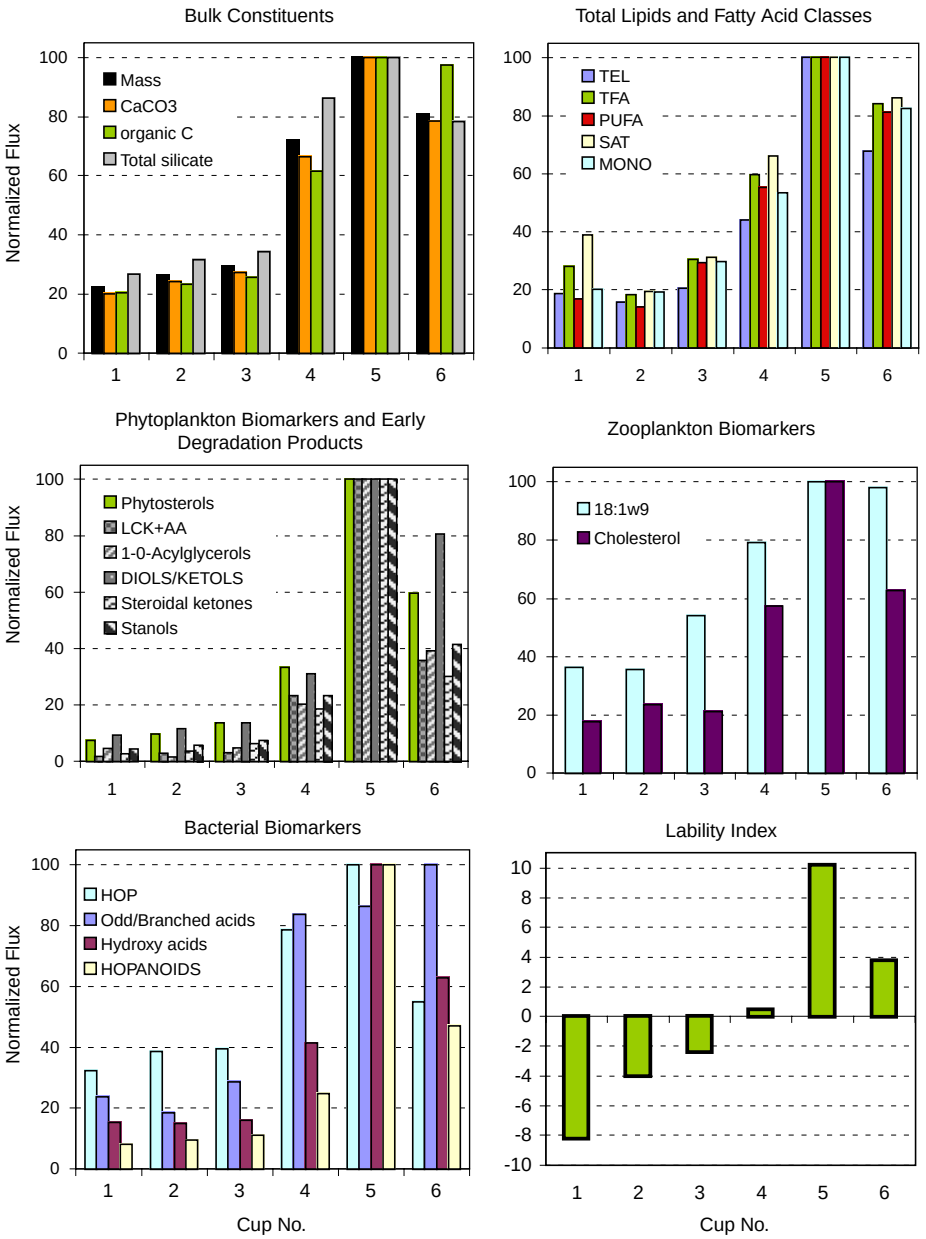

Fig. 7. Normalized fluxes of bulk constituents and diagnostic lipid biomarkers and changes in the LI of the organic material in the trap cup. The collection dates for the trap cups and shorthand notations are given in Table 2. The flux data (Table 3) have been scaled as a percentage of the maximum flux measured over the time period. The LI is calculated from the composition of key biomarkers, as described in the text.

the most rapidly settling material from this bloom/flux event in Cup 3 (November 18–December 2), this material would have retained a higher percentage of PUFAs originally present. This would cause the peak flux of PUFAs to lead the flux peaks of longer-lived phytoplankton biomarkers. Inputs of very rapidly settling material at the onset of the event are supported by observations

of large greenish brown "clumps" of fibrous material, possibly the remains of gelatinous zooplankton fecal pellets, in Cup 3 and Cup 4 (N. Ralph, pers. observ.). A significant fraction of the deep PUFA flux observed at the onset of the event might also reflect increased inputs of zooplankton biomass remains from zooplankton predation and "sloppy feeding" (e.g., Vinogradov, 1962; Urrere and Knauer, 1981; Bishop et al., 1986b). An increase in zooplankton-derived flux is also suggested by flux increases of cholesterol and 18:1ω9, both of which are also enriched in animal tissues (e.g., Sargent and Whittle, 1981; Bühring and Christiansen, 2001) in Cup 3.

In contrast to more labile biomarkers, flux patterns of the hopanone 22,29,30 tris-*nor*hopan-21-one and odd and branched fatty acids were similar to those of the bulk components. These compounds (and cholesterol) are the major extractable lipid biomarkers in material collected during low flux periods, and appear to be indicative of a highly refractory organic residue (Conte et al., 1998a; Kiriakoulakis et al., 2001). The coincident increase in the flux of these resistant biomarkers with the initial increase in mass flux in Cup 4 suggests that at the onset of the pulsed flux event, much of the material comprising the deep flux is not derived from surface production, but rather from biological aggregation of more refractory suspended particles. This conclusion is consistent with the alkenone evidence presented above for a "scavenged flux" component.

5. Discussion

Our results show the very significant impact of a warm, mesoscale feature as coupled with wind forcing on the export of labile bioreactive material to the deep ocean. The present data suggest that when the abrupt increase in 3200 m flux was observed, a highly productive mesoscale feature with mixing depths of >180 m was passing across the deep trap's catchment area. Although the limited spatial coverage precludes a detailed characterization of the feature and its physical dynamics, the presence of this feature for approximately 1 month at the BTM mooring site and the magnitude of the 3200 m flux increase, suggests that it was a mesoscale phenomenon.

5.1. Implications for controls on export flux and remineralization depth profiles

The results presented here and in Conte et al. (1998a) clearly demonstrate that fluxes at a particular site in the deep oligotrophic ocean exhibit extreme temporal variability in both quantity and composition on time scales of days to weeks. Large, episodic pulses of relatively fresh biogenic material have also been observed at shallower depths in the oligotrophic NE Atlantic closer to ocean margins (Fischer et al., 1996).

Physical forcing of upper ocean primary production by eddies and rapid sedimentation to the deep ocean has previously been observed in the Arabian Sea (Dickey et al., 1998b; Honjo et al., 1999). Our results extend this observation to further show that warm, mesoscale circulation features that perturb mixed layer dynamics, coupled with short-lived meteorological forcing, may also generate transient upper ocean conditions that stimulate phytoplankton production and enhance export flux.

The relative importance of increased productivity generated by nutrient influx (either horizontal or vertical) versus the increased depth of vertical mixing for enhancement of export flux is not known. The thick warm thermostad of the feature examined in this study clearly promoted a situation where the depth of mixing could suddenly increase by >100 m when surface stratification was eroded by seasonal cooling. This led to nearly immediate penetration of the nutricline in the feature, whereas in the surrounding waters a more slowly deepening mixed layer would result in more gradual nutrient entrainment. Evidence for weak stratification in some chlorophyll fluorescence profiles as well as variable air temperature and wind speed suggest intermittent mixing. In a weakly stabilized water column, alternating episodes of mixing and stratification can be forced by variable heat flux and wind intensity associated with the passage of weather systems. Previous studies of warm-core Gulf Stream rings have

shown that such variability is mixed layer structure, which is on the order of days, maintains nutrient supply to enhance phytoplankton production while the transient episodes of mixed layer destratification subsequently export phytoplankton material into the subeuphotic zone waters, enhancing export fluxes (Smith and Baker, 1985; Bishop et al., 1986a).

The effect of mesoscale or other advecting features on perturbation of mixed layer dynamics is likely to vary seasonally. During summer periods of strong thermal stratification, a thick isothermal lens would have little influence on mixed layer depth, whereas during periods of developing stratification or destratification or low mixed layer stability, the effect of such features on the depth of mixing may be substantial, as described here. This could be one explanation for the observation that large changes in mass flux in the OFP biweekly record are most commonly observed in the December–March period.

The importance of a given mesoscale feature on export flux is also likely to vary as the feature ages with physical evolution and biological succession. Sweeney et al. (in press) present a conceptual model of the sequential development of biological conditions in cyclonic and mode water eddies as they age. During the initial eddy intensification phase, nutrient upwelling supports enhanced primary production. This is followed by a period of enhanced secondary production and export as eddy rotation relaxes. Alternatively, there is some evidence (e.g., Roman et al., 1995) to suggest that vertically migrating zooplankton may locate and congregate in high productivity surface features. Although we have no information on the initiation or time course of the feature discussed here, the high zooplankton biomass observed in the central waters of this feature indicates that it was sufficiently mature to establish a zooplankton community that was distinct from the surrounding waters.

Models and advanced analytical methods are clearly needed to help us understand the impact of mesoscale features, coupled with transient meteorological forcing, on biogeochemical cycles and budgets on basin and global scales (e.g., Garçon et al., 2001; Williams and Follows, 2002). Recently, researchers have utilized regional numerical model simulations as well as satellite altimetry data in conjunction with statistical models to estimate vertical displacement of isopycnal surfaces and the fraction of the annual North Atlantic Ocean nutrient budget supplied by mesoscale eddies (e.g., McGillicuddy et al., 1998; Oschlies and Garçon, 1998; Siegel et al., 1999). Some of these approaches suggest that eddy induced-upwelling may be sufficient to cause nitrate injections into the euphotic layer to a degree sufficient to balance the nutrient demand implied by other geochemical estimates of new production. However, this hypothesis remains controversial and unresolved at the moment (e.g., see differing viewpoints presented in McGillicuddy et al., 1998; Oschlies and Garçon, 1998; and also review of Lewis, 2002). An often used assumption has been that first baroclinic mode cyclonic eddies dominate the statistics and thus the biogeochemical variability. While it appears that first baroclinic mode cyclonic eddies occur much more frequently than higher mode eddies, questions remain concerning the relative biogeochemical importance of the various types of eddies. For example, BTM and OFP data sets tend to indicate that not all first baroclinic mode cyclonic eddies lead to enhancement of nutrient fluxes, primary production, and carbon flux to depth. We hypothesize that dependencies such as the ages of eddies (e.g., Flierl and McGillicuddy, 2002; Sweeney et al., in press) and conditions during eddy passage such as local wind forcing and ambient stratification (i.e., synoptic-scale seasonal, interannual, and decadal effects) during eddy passage play important roles in determining whether nitrate enhancement takes place and if so to what degree.

Interestingly, two of the most impressive mesoscale events of the past decade occurred at the BTM/OFP sites in the summer of 1995 and the autumn of 1996. Both were characterized by extremely high biomass and particle flux. The 1995 event was a second baroclinic mode eddy ('mode' eddy type; McNeil et al., 1999) and the 1996 fall event was the warm mesoscale feature described in this work. Our data sets indicate that neither of these types of features is unusual, nor do they lend themselves to application of a simple first

baroclinic mode-satellite altimetry analysis. Analytical approaches and models that do not account for enhanced nutrients for non-first baroclinic mode eddies or coupled surface forcing would underestimate contributions from these other eddy types. Effects of phytoplankton species successions in eddies and carbon transformation and transport processes (e.g., biological pump) are likely to be important as well and remain to be explored with eddy models.

It is also worth noting that remote sensing of eddies via sea-surface temperature and color can be useful, but it is also problematic because of missing data caused by cloud obscuration and the inability to sample subsurface chlorophyll maxima. As seen here (cf. Fig. 4c) and in warm-core rings (e.g., Bishop et al., 1986a, b), surface chlorophyll measurements may not be representative of total water column integrated chlorophyll concentration when intermittently mixing thick thermostad layers are present.

5.2. *Implications for the biological reprocessing of particle flux in the water column*

Substantial differences were observed in the temporal phasing of trap components, indicating a temporal evolution in deep flux dynamics. For this flux event, the increase in the flux of bulk components, especially the residual silicate fraction, and the flux of refractory organic compounds clearly preceded the main pulse of the labile, surface-derived phytoplankton detritus. The coincident increase in the flux of refractory and zooplankton-derived compounds suggests that in the initial stage of the deep flux event, the mass flux increased largely as a result of an increase in the flux of refractory materials scavenged from the water column and repackaged into sinking particles and increased zooplankton inputs; in the later stage of the event, bloom products, partially reprocessed by animals and microbes, dominated the flux.

Conte et al. (2001a) have shown that there is a strong coherence and lack of any appreciable time lag in the 500, 1500 and 3200 mass flux records at the OFP site. They hypothesized that this may be due to an initial increase in large particle production by deep-dwelling zooplankton at the beginning of a flux event caused by the stimulation of grazer scavenging activity when particles of high nutritional value are encountered. Although little is known about feeding behavior for midwater animals, existing data on feeding behavior in epipelagic animals (e.g., Paffenhofer and Van Sant, 1985; Deibel, 1998; Flood and Deibel, 1998) indicate that scavenging activities and, in turn, particle aggregation rates are modulated by the nutritive quality of particles encountered.

Several direct lines of evidence also indicate that midwater animals effectively reprocess sinking particles as they transit through the water column. This includes observations of large changes in fecal pellet flux and composition over short depth intervals (Urrere and Knauer, 1981; Karl and Knauer, 1984; Bishop et al., 1986a, b), seasonally variable fluxes of ^{230}Th (Bacon et al., 1985), midwater ^{234}Th deficits (Benitez-Nelson et al., 2001), midwater concentration and flux maxima of zooplankton-derived compounds (e.g., Wakeham et al., 1984; Conte and Bishop, 1988; Conte, 1989; Wakeham et al., 1997), and rapid homogenization of the bulk composition of the sinking particle flux between 500 and 1500 m at the OFP site (Conte et al., 2001a).

Non-selective gelatinous filter feeders such as appendicularia and salps are important components of mesopelagic ecosystems and may have a particularly large influence on particle flux (Fenaux et al., 1998; Madin and Deibel, 1998; Andersen, 1998). Appendicularia agglutinate particles that range in size from 0.2 to hundreds of microns during feeding (Madin and Deibel, 1998; Andersen, 1998; Flood and Deibel, 1998). Their filtration "houses", which are shed and expanded every several hours, sink rapidly and are often identifiable in the OFP traps (M. Conte, pers. observ.).

Salp fecal pellets are also commonly observed in the OFP traps (M. Conte, pers. observ.). Salp species include strong vertical migrators and seasonal or permanent non-migratory mesopelagic residents. Salps also feed on a large range of particle sizes and have relatively low (30–60%) assimilation efficiencies (Madin and Deibel, 1998; Andersen, 1998; and references therein). Salp fecal

pellets contain significant concentrations of particulate aluminum and radionuclides, indicating efficient aggregation of lithogenic materials as well as organic particles. Salp fecal pellets sink at rates of 300–2700 m d^{-1} and thus can rapidly transport of labile, undegraded material to depth (Andersen, 1998). Salp pellets also rapidly decompose and disagregate as they sink (Andersen, 1998).

Our results furthermore imply that biological reprocessing of flux material within the water column acts to increase the temporal coupling between the surface and deep ocean environments. Conte et al. (1998a) hypothesized that the rapid sinking and disaggregation of salp fecal pellets and similarly sized biogenic particles containing labile organic material would recharge the deep-water column with relatively undegraded particles of high nutritive value, and thereby stimulate the feeding activities of organisms that aggregate particles within the water column. The observations here are consistent with this model.

6. Conclusions

The major conclusion of this study is that the important processes that control flux to the deep ocean are often episodic in nature and driven by the interactions between mesoscale variability and upper ocean dynamics. While the overall contribution of short-lived, transient physical forcing to export flux of bioreactive carbon and associated elements on longer time scales is not known, the OFP time-series data suggest that transient upper ocean forcing could be the trigger responsible for a sizeable fraction of the total deep ocean flux. If so, the statistics of such forcing will control, in part, remineralization depth profiles and food supply in the meso- and bathypelagic realms. The statistics of infrequent events are significantly more dependent on system variability than its mean (e.g., Katz and Brown, 1992; Wagner, 1999; Overland et al., 2000), and furthermore the more extreme the event, the greater the influence of underlying variability of controlling factors (e.g., Dubrovsky et al., 2000). The implication for models that strive to predict the ocean's response to different climate change scenarios is that the high-frequency temporal and mesoscale and submesoscale spatial variability of the climate–ocean system must be better characterized.

The transparency of the mesoscale feature discussed here to TOPEX and ERS altimetry also emphasizes that altimetry-based biogeochemical models that focus only on first baroclinic mode eddies and do not incorporate short-term variability in meteorological forcing are likely to be inadequate to fully characterize the biogeochemical consequences of upper ocean physical variability. Our results and those of McNeil et al. (1999) show that in areas with significantly complex vertical structure (e.g., second baroclinic mode and higher) and likely short horizontal coherence scales, in situ measurements of key parameters over the requisite space and time scales, are required. New sensor technologies and more comprehensive spatial coverage by moorings (e.g., Lewis, 2002), gliders, autonomous underwater vehicles, and floats capable of measuring high-frequency non-seasonal variability as well as expanded remote sensing capabilities are needed to provide key data sets for future analytical and modeling efforts in this area. In particular, this sampling strategy used with data assimilation modeling offers promise for discriminating local versus advective effects.

Our data also provide further evidence that midwater zooplankton play an important role in modulating the downward flux of material and energy and in coupling the surface and deep ocean environments. Although it has been universally recognized that export fluxes are strongly modified and attenuated in the upper 1500 m, little is known about how mesopelagic ecosystems influence or are affected by particle flux dynamics, or how interactions between vertical migrators and mesopelagic predators affect the downward flux of materials. Clearly, these are important areas for future study.

Finally, it cannot be overemphasized that long-term sustained measurement programs are essential for understanding how ocean biogeochemical processes operate on time scales ranging from days to decades. In the future, the ability to extend temporally and vertically well-resolved measurements over horizontal domains on the order of

100–200 km at the Bermuda time-series site will allow more definitive conclusions to be made as to the origins and physical dynamics of meso- and submesoscale features and their resultant effects on biogeochemical fluxes.

Acknowledgements

The Oceanic Flux Program has been supported by the National Science Foundation Chemical Oceanography program (most recently by OCE-9986038 and OCE-971703 to M. Conte) and we thank the Chemical Oceanography program for their continued support. Organic geochemical research has been supported by Penzance Funds, the Mellon Foundation and the Woods Hole Oceanographic Institution. Werner Deuser initiated the OFP time-series and was its Principal Investigator from 1978–1994; his contributions to the pre-1995 record are acknowledged. We also thank E. Ross, L. Christman and N. Ralph for their technical assistance, and S. Sylva for his assistance with the GCMS analyses. The BTM has been supported by the National Science Foundation Ocean Technology and Interdisciplinary Coordination Program, Chemical Oceanography Program, and Oceanographic Instrumentation and Technical Service Program (TD: OCE-9627281, OCE-9730471, OCE-9819477), National Aeronautics and Space Administration Program (TD: NAGW-3949, NAS5-97127), the National Ocean Partnership Program (TD: N40000149810803), the Office of Naval Research Ocean Engineering and Marine Systems Program (DF: N00014-96-1-0028), the University of California, Santa Barbara (to T. Dickey, UCSB), and gifts from the Vettleson Foundation and the Andrew W. Mellon Foundation (to BBSR). Songnian Jiang kindly provided analytical and computational support for this paper. Financial support for the BATS program has been provided primarily from the NSF through the US Joint Global Ocean Flux Study (grants OCE 93-01950 and OCE96-117795 for the study period). We thank the many scientists and technicians of the BATS program, who have contributed to these data and analyses. Special thanks are also extended to Butch Stovell for his expert assistance on OFP mooring cruises for many years, to John Kemp, Derek Manov, and Frank Spada for their dedication to the BTM mooring activity, and to the crew of the R./V. *Weatherbird II* for their assistance at sea. We also thank Marlon Lewis, Roger Summons and an anonymous reviewer for helpful comments that improved the manuscript. This is WHOI contribution number 10895 and US JGOFS Contribution Number 834.

References

Al-Mutari, H., Landry, M.R., 2001. Active export of carbon and nitrogen at Station ALOHA by diel migrant zooplankton. Deep-Sea Research II 48, 2083–2103.

Andersen, V., 1998. Salp and pyrosomid blooms and their importance in biogeochemical cycles. In: Bone, Q. (Ed.), The Biology of Pelagic Tunicates. Oxford University Press, Oxford, pp. 125–138.

Bacon, M.P., Huh, C.-A., Fleer, A.P., Deuser, W.G., 1985. Seasonality in the flux of natural radionuclides and plutonium in the deep Sargasso Sea. Deep-Sea Research 32, 273–286.

Barrett, S.M., Volkman, J.K., Dunstan, G.A., LeRoi, J.M., 1995. Sterols of 14 species of marine diatoms (Bacillariophyta). Journal of Phycology 31, 360–369.

Benitez-Nelson, C., Buesseler, K.O., Karl, D.M., Andrews, J., 2001. A time-series study of particulate matter export in the North Pacific Subtropical Gyre based on ^{234}Th:^{238}U disequilibrium. Deep-Sea Research I 48, 2595–2611.

Bijma, J., Altabet, M., Conte, M., Kinkel, H., Versteegh, J.M., Volkman, J.K., Wakeham, S.G., Weaver, P.P., 2001. Primary signal: ecological and environmental factors—report from Working Group 2. Geochemistry, Geophysics and Geosystems 2, paper number 2000GC000051.

Billett, D.S.M., Lampitt, R.S., Rice, A.L., Mantoura, R.F.C., 1983. Seasonal sedimentation of phytoplankton to the deep-sea benthos. Nature 302, 520–522.

Bishop, J.K.B, Conte, M.H., Wiebe, P.H., Roman, M.R., Langdon, C., 1986a. Particulate matter production and consumption in deep mixed layers: observations in a warm-core ring. Deep-Sea Research 33, 1813–1841.

Bishop, J.K.B, Stepien, J.C., Wiebe, P.H., 1986b. Particulate matter distributions, chemistry and flux in the Panama Basin: response to environmental forcing. Progress in Oceanography 17, 1–59.

Björkhem, I., Gustafsson, J.-A., 1971. Mechanism of microbial transformation of cholesterol into coprostanol. European Journal of Biochemistry 21, 428–432.

Bordier, C.G., Sellier, N., Foucault, A.P., LeGoffic, F., 1996. Purification and characterization of deep sea shark *Centrophorous squamosus* liver oil 1-*O*-alkylglycerol ether lipids. Lipids 31, 521–528.

Bradshaw, S.A., Eglinton, G., 1993. Marine invertebrate feeding and the sedimentary lipid record. In: Engel, M.H., Macko, S.A. (Eds.), Organic Geochemistry, Principles and Applications. Plenum Press, New York, pp. 225–235.

Bühring, S.I., Christiansen, B., 2001. Lipids in selected abyssal benthopelagic animals: links to the epipelagic zone? Progress in Oceanography 50, 369–382.

Chavez, F.P., Smith, S.L., 1995. Biological and chemical consequences of upper ocean upwelling. In: Summerhayes, C., Emeis, K.-C., Angel, M.V., Smith, R.L., Zeitzschel, B. (Eds.), Upwelling in the Ocean: Modern Processes and Ancient Consequences. Wiley, New York, pp. 149–170.

Chelton, D.B., Bernla, P.A., McGowan, J.A., 1982. Large-scale physical and biological interaction in the California Current. Journal of Marine Research 40, 1095–1125.

Conte, M.H., 1989. The biogeochemistry of particulate lipids in warm-core gulf stream ring systems. Ph.D. Thesis, Columbia University, 584pp.

Conte, M.H., Bishop, J.K.B., 1988. Nanogram quantification of nonpolar lipid classes in environmental samples by high performance thin layer chromatography. Lipids 23, 493–500.

Conte, M.H., Eglinton, G., Madureira, L.A.S., 1992. Long-chain alkenones and alkyl alkenoates as palaeotemperature indicators: their production, flux, and early diagenesis in the eastern North Atlantic. In: Eckardt, C.B., Larter, S.R. (Eds.), Advances in Organic Geochemistry 1991. Organic Geochemistry 19, 287–298.

Conte, M.H., Volkman, J.K., Eglinton, G., 1994. Lipid biomarkers of the Prymnesiophyceae. In: Green, J.C., Leadbetter, B.S.C. (Eds.), The Haptophyte Algae. Clarendon Press, Oxford, pp. 351–377.

Conte, M.H., Eglinton, G., Madureira, L.A.S., 1995. Origin and fate of organic biomarker compounds in the water column and sediments of the eastern North Atlantic. Philosophical Transactions of the Royal Society 348, 169–178.

Conte, M.H., Weber, J.C., Ralph, N., 1998a. Episodic particle flux in the deep Sargasso Sea: an organic geochemical assessment. Deep-Sea Research I 45, 1819–1841.

Conte, et al., 1998b. Genetic and physiological influences on the alkenone/alkenoate versus growth temperature relationship in *Emiliania huxleyi* and *Gephyrocapsa oceanica*. Geochimica et Cosmochimica Acta 62, 51–68.

Conte, M.H., Ralph, N., Ross, E., 2001a. Seasonal and interannual variability in deep ocean particle fluxes at the Oceanic Flux Program/Bermuda Atlantic Time-series (BATS) site in the western Sargasso Sea near Bermuda. Deep-Sea Research II 48, 1471–1505.

Conte, M.H., Weber, J.C., King, L.L., Wakeham, S.G., 2001b. The alkenone temperature signal in western North Atlantic surface waters. Geochimica et Cosmochimica Acta 65, 4275–4287.

Dam, H.G., Roman, M.R., Youngbluth, M.J., 1995. Downward export of respiratory carbon and dissolved inorganic nitrogen by diel-migrant mesozooplankton at the JGOFS Bermuda time-series station. Deep-Sea Research II 42, 1187–1197.

Deibel, D., 1998. Feeding and metabolism of appendicularia. In: Bone, Q. (Ed.), The Biology of Pelagic Tunicates. Oxford University Press, Oxford, pp. 139–149.

DeLeeuw, J.W., Rijpstra, W.I.C., Schenck, P.A., 1981. The occurrence and identification of C_{30}, C_{31} and C_{32} alkan-1, 15-diols and alkan-15-one-1-ols in Unit I and Unit II Black Sea sediments. Geochimica Cosmochimica Acta 45, 2281–2285.

DeLeeuw, J.W., Rijpstra, W.I.C., Nienhuis, P.H., 1995. Free and bound fatty acids and hydroxy fatty acids in the living and decomposing eelgrass *Zostera marina* L. Organic Geochemistry 23, 721–728.

Deuser, W.G., 1986. Seasonal and interannual variations in deep-water particle fluxes in the Sargasso Sea and their relation to surface hydrography. Deep-Sea Research 33, 225–246.

Deuser, W.G., 1996. Temporal variability of particle flux in the deep Sargasso Sea. In: Ittekkot, V., Honjo, S., Depetris, P.J. (Eds.), Particle Flux in the Deep Ocean. Wiley, New York, pp. 185–198.

Deuser, W.G., Ross, E.H., Anderson, R.F., 1981. Seasonality in the supply of sediment to the deep Sargasso Sea and implications for the rapid transfer of matter to the deep ocean. Deep-Sea Research 28, 495–505.

Deuser, W.G., Muller-Karger, F.E., Evans, R.H., Brown, O.B., Esaias, W.E., Feldman, G.C., 1990. Surface-ocean color and deep-ocean carbon flux: how close a connection? Deep-Sea Research 37, 1331–1343.

Deuser, W.G., Jickells, T.D., King, P., Commeau, J.A., 1995. Decadal and annual changes in biogenic opal and carbonate fluxes to the deep Sargasso Sea. Deep-Sea Research I 42, 1923–1932.

Dickey, T., Falkowski, P., 2002. Solar energy and its biological–physical interaction in the sea. In: Robinson, A.R., McCarthy, J.J., Rothschild, B.J. (Eds.), The Sea, Vol. 12. Wiley, New York, pp. 401–440.

Dickey, T., Marra, J., Stramska, M., Langdon, C., Granata, T., Weller, R., Plueddemann, A., Yoder, J., 1994. Bio-optical and physical variability in the sub-arctic North Atlantic Ocean during the spring of 1989. Journal of Geophysical Research 99, 22541–22556.

Dickey, T., Frye, D., Jannasch, H., Boyle, E., Manov, D., Sigurdson, D., McNeil, J., Stramska, M., Michaels, A., Nelson, N., Siegel, D., Chang, G., Wu, J., Knap, A., 1998a. Initial results from the Bermuda Testbed Mooring program. Deep-Sea Research I 45, 771–794.

Dickey, T., Marra, J., Sigurdson, D.E., Weller, R.A., Kinkade, C.S., Zedler, E., Wiggert, J.D., Langdon, C., 1998b. Seasonal variability of bio-optical and physical properties in the Arabian Sea: October 1994–October 1995. Deep Sea Research II 45, 2001–2025.

Dickey, T., Frye, D., McNeil, J., Manov, D., Nelson, N., Sigurdson, D., Jannasch, H., Siegel, D., Michaels, T., Johnson, R., 1998c. Upper-ocean temperature response to Hurricane Felix as measured by the Bermuda Testbed Mooring. Monthly Weather Review 126, 1195–1201.

Dickey, T., Zedler, S., Yu, X., Doney, S.C., Frye, D., Jannasch, H., Manov, D., Sigurdson, D., McNeil, J.D.,

Dobeck, L., Gilboy, T., Bravo, C., Siegel, D.A., Nelson, N., 2001. Physical and biogeochemical variability from hours to years at the Bermuda Testbed Mooring site: June 1994–March 1998. Deep-Sea Research II 48 (8–9), 2105–2140.

Dickson, R.R., Lazier, J., Meincke, J., Rhines, P., 1996. Long-term coordinated changes in the convective activity of the North Atlantic. Progress in Oceanography 38, 241–295.

Diercks, A.-R., Asper, V.L., 1997. In situ settling speeds of marine snow aggregates below the mixed layer: Black Sea and Gulf of Mexico. Deep-Sea Research I 44, 385–398.

Dubrovsky, M., Zalud, Z., Stastna, M., 2000. Sensitivity of CERES-Maize yields to statistical structure of daily weather series. Climatic Change 46, 447–472.

Fang, J., Barcelona, M.J., Nogi, Y., Kato, C., 2000. Biochemical implications and geochemical significance of novel phospholipids of the extremely barophilic bacteria from the Marianas Trench at 11000 m. Deep-Sea Research I 47, 1173–1182.

Fenaux, R., Bone, Q., Deibel, D., 1998. Appendicularian distribution and zoogeography. In: Bone, Q. (Ed.), The Biology of Pelagic Tunicates. Oxford University Press, Oxford, pp. 251–264.

Fischer, G., Neuer, S., Krause, G., Wefer, G., 1996. Short-term sedimentation pulses recorded with a fluorescence sensor and sediment traps in 900 m water depth in the Canary Basin. Limnology and Oceanography 41, 1354–1359.

Flierl, G., McGillicuddy Jr., D.J., 2002. Mesoscale and submesoscale physical-biological interactions. In: Robinson, A.R., McCarthy, J.J., Rothschild, B.J. (Eds.), Biological-physical Interactions in the sea, The sea, Vol. 12. Wiley, New York, pp. 113–185.

Flood, P.R., Deibel, D., 1998. The appendicularian house. In: Bone, Q. (Ed.), The Biology of Pelagic Tunicates. Oxford University Press, Oxford, pp. 105–124.

Gagosian, R.B., Smith, S.O., Lee, C., Farrington, J.W., Frew, N.M., 1980. Steroid transformations in recent marine sediments. In: Douglas, A.G., Maxwell, J.R. (Eds.), Advances in Organic Geochemistry. Pergamon Press, Oxford, pp. 407–419.

Garçon, V.C., Oschlies, A., Doney, S.C., McGillicuddy, D., Waniek, J., 2001. The role of mesoscale variability on plankton dynamics in the North Atlantic. Deep-Sea Research I 48, 2199–2226.

Gaskell, S.J., Eglinton, G., 1975. Rapid hydrogenation of sterols in a contemporary lacustrine sediment. Nature 254, 209–211.

Gehlen, M., Rabouille, C., Ezat, U., Guidi-Guilvard, L.D., 1997. Drastic changes in deep-sea sediment porewater composition induced by episodic input of organic matter. Limnology and Oceanography 42, 980–986.

Gelin, F., Volkman, J.K., deLeeuw, J.W., Sinninghe-Damsté, J.S., 1997. Mid-chain hydroxy long-chain fatty acids in microalgae from the genus *Nannochloropsis*. Phytochemistry 45, 641–646.

Gillan, F.T., Johns, R.B., 1986. Chemical markers for marine bacteria: fatty acids and pigments. In: Johns, R.B. (Ed.), Biological Markers in the Sedimentary Environment. Elsevier Press, New York, pp. 291–309.

Glover, D.M., Doney, S.C., Mariano, A.J., Evans, R.H., McCue, S.J., 2002. Mesoscale variability in time-series data: satellite based estimates for the U.S. JGOFS Bermuda Atlantic Time-series study (BATS) site. Journal of Geophysical Research, 107, 3092 doi:10.1029/2000JC000589.

Gooday, A.J., Turley, C.M., 1990. Response by benthic organisms to inputs of organic material to the ocean floor: a review. Philosophical Transactions of the Royal Society of London A 331, 119–138.

Goosens, H., Rijpstra, W.I.C., Duren, R.R., deLeeuw, J.W., Schenck, P.A., 1986. Bacterial contribution to sedimentary organic matter; a comparative study of lipid moieties in bacteria and recent sediments. Organic Geochemistry 10, 683–696.

Graf, G., 1989. Benthic–pelagic coupling in a deep-sea benthic community. Nature 341, 437–439.

Granata, T., Wiggert, J., Dickey, T., 1995. Trapped near-inertial waves and enhanced chlorophyll distributions. Journal of Geophysical Research 100, 20793–20804.

Haidar, A.T., Thierstein, H.R., 2001. Coccolithophore dynamics off Bermuda (N. Atlantic). Deep-Sea Research II 48, 1925–1956.

Harvey, H.R., Bradshaw, S.A., O' Hara, S.C.M., Corner, E.D.S., 1987. Biotransformation and assimilation of dieteary lipids by *Calanus* feeding on a dinoflagellate. Geochimica et Cosmochimica Acta 51, 3031–3040.

Harwood, J.L., Russell, N.J., 1984. Lipids in Plants and Microorganisms. George Allen & Unwin, London, 162pp.

Honjo, S., Dymond, J., Prell, W., Ittekot, V., 1999. Monsoon-controlled export fluxes to the interior of the Arabian Sea. Deep-Sea Research II 46, 1859–1902.

Ikekawa, N., 1985. Structures, biosynthesis and function of sterols in invertebrates. In: Danielsson, H., Sjövall, J. (Eds.), Sterols and Bile Acids. Elsevier Science Publishers Biomedical Division, Amsterdam, pp. 199–213.

Jantzen, E., Bryn, K., 1985. Whole-cell and lipopolysaccharide fatty acids and sugars of gram-negative bacteria. In: Goodfellow, M., Minnikin, D.E. (Eds.), Chemical methods in bacterial systematics. Academic Press, London, pp. 145–171.

Jiang, S., Dickey, T., Madin, L.M. Estimation of zooplankton biomass temporal variability from ADCP backscatter time series data at the Bermuda Testbed Mooring site. Deep-Sea Research I, submitted for publication.

Joyce, T.M., Robbins, P., 1996. The long-term hydrographic record at Bermuda. Journal of Climate 9, 3121–3131.

Kaneda, T., 1991. *Iso* and *anteiso*-fatty acids in bacteria: biosynthesis, function, and taxonomic significance. Microbiological Reviews 55, 288–302.

Karl, D.M., Knauer, G.A., 1984. Vertical distribution, transport, and exchange of carbon in the northeast Pacific Ocean: evidence for multiple zones of biological activity. Deep-Sea Research 31, 221–243.

Karl, D.M., Christian, J.R., Dore, J.E., Hebel, D.V., Letelier, R.M., Tupas, L.M., Winn, C.D., 1996. Seasonal and interannual variability in primary production and particle flux at Station ALOHA. Deep-Sea Research II 43, 539–568.

Karl, D.M., Bidigare, R.R., Letelier, R.M., 2001. Long-term changes in plankton community structure and productivity in the North Pacific Subtropical Gyre: the domain shift hypothesis. Deep-Sea Research II 48, 1449–1470.

Kattner, G., Hagen, W., Albers, C., 1998. Exceptional lipids and fatty acids in the pteropod *Clione limacina* (Gastropoda) from both polar oceans. Marine Chemistry 61, 219–228.

Katz, R.W., Brown, B.G., 1992. Extreme events in a changing climate: variability is more important than averages. Climatic Change 21, 289.

Kiriakoulakis, K., Stutt, E., Rowland, S.J., Vangriesheim, A., Lampitt, R.S., Wolff, G.A., 2001. Controls on the organic chemical composition of settling particles in the Northeast Atlantic Ocean. Progress in Oceanography 50, 65–87.

Konstadinos, K., Stutt, E., Rowland, S.J., Vangriesheim, A., Lampitt, R.S., Wolff, G.A., 2001. Controls on the organic chemical composition of settling particles in the Northeast Atlantic Ocean. Progress in Oceanography 50, 65–87.

Lampitt, R.S., 1985. Evidence for the seasonal deposition of detritus to the deep-sea floor and its subsequent resuspension. Deep-Sea Research 32, 885–897.

Lewis, M.R., 2002. Variability of plankton and plankton processes on the mesoscale. In: Williams, P.J.le.B., Thomas, D.N., Reynolds, C.S. (Eds.), Phytoplankton Productivity: Carbon Assimilation in Marine and Freshwater Ecosystems. Blackwell Science, Oxford, pp. 141–155.

Madin, L.P., Deibel, D., 1998. Feeding and energetics of Thaliacea. In: Bone, Q. (Ed.), The Biology of Pelagic Tunicates. Oxford University Press, Oxford, pp. 81–104.

Madin, L.P., Horgan, E.F., Steinberg, D.K., 2001. Zooplankton at the Bermuda Atlantic Time-series Study (BATS) station: diel, seasonal and interannual variation in biomass, 1994–1998. Deep-Sea Research II 48, 2063–2082.

Mansour, M.P., Volkman, J.K., Jackson, A.E., Blackburn, S.I., 1999. The fatty acid and sterol composition of five marine dinoflagellates. Journal of Phycology 35, 710–720.

Marlowe, I.T., 1984. Lipids as palaeoclimatic indicators. Ph.D. Thesis, University of Bristol, UK, 273pp.

Marra, J., Dickey, T.D., Ho, C., Kinkade, C.S., Sigurdson, D.E., Weller, R.A., Barber, R.T., 1998. Variability in primary production as observed from moored sensors in the central Arabian Sea in 1995. Deep-Sea Research II 45, 2253–2267.

McGillicuddy, D.J., Kosnyrev, V.K., 2001. Dynamical interpolation of mesoscale flows in the topex/poseidon diamond surrounding the US JGOFS Bermuda Atlantic Time-series site. Journal of Geophysical Research 106, 16641–16656.

McGillicuddy, D.J., Robinson, A.R., 1997. Eddy-induced nutrient supply and new production in the Sargasso Sea. Deep-Sea Research I 44, 1427–1450.

McGillicuddy, D.J., Robinson, A.R., Siegel, D.A., Jannasch, H.W., Johnson, R., Dickey, T.D., McNeil, J.D., Michaels, A.F., Knap, A.H., 1998. Influence of mesoscale eddies on new production in the Sargasso Sea. Nature 394, 263–266.

McGillicuddy, D.J., Robinson, R., Siegel, D.A., Michaels, A.F., Bates, N.R., Knap, A.H., 1999. Mesoscale variations in biogeochemical properties in the Sargasso Sea. Journal of Geophysical Research 104, 13381–13394.

McGillicuddy Jr., D.J., Kosnyrev, V.K., Ryan, J.P., Yoder, J.A., 2001. Covariation of mesoscale ocean color and sea-surface temperature patterns in the Sargasso Sea. Deep-Sea Research II 48, 1823–1836.

McNeil, J.D., Jannasch, H.W., Dickey, T., McGillicuddy, D., Brzezinski, M., Sakamoto, C.M., 1999. New chemical, bio-optical, and physical observations of upper ocean response to the passage of a mesoscale eddy off Bermuda. Journal of Geophysical Research 104, 15537–15548.

Mermoud, F.L., Wunsche, L., Clerc, O., Gulacar, F.O., Buchs, A., 1984. Steroidal ketones in the early diagenetic transformations of Δ^5 sterols in different types of sediments. Organic Geochemistry 6, 25–29.

Michaels, A.F., Knap, A.H., 1996. Overview of the US JGOFS Bermuda Atlantic Time-series Study (BATS) and the hydrostation S program. Deep-Sea Research II 43, 157–198.

Nelson, M.M., Phleger, C.F., Mooney, B.D., Nichols, P.D., 2000. Lipids of gelatinous Antarctic zooplankton: Cnideria and Ctenophora. Lipids 35, 551–559.

Nelson, N.B., 1998. Spatial and temporal extent of sea surface temperature modifications by hurricanes in the Sargasso Sea during the 1995 season. Monthly Weather Review 126, 1364–1368.

Newton, P.P., Lampitt, R.S., Jickells, T.D., King, P., Boutle, C., 1994. Temporal and spatial variability of biogenic particle fluxes during JGOFS northeast Atlantic process studies at 47°N 20°W. Deep-Sea Research I 41, 1617–1642.

Nishimura, M., Koyama, T., 1977. The occurrence of stanols in various living organisms and the behaviour of sterols in contemporary sediments. Geochimica et Cosmochimica Acta 41, 379–385.

Oschlies, A., Garçon, V.C., 1998. Eddy-induced enhancement of primary production in a model of the North Atlantic Ocean. Nature 394, 266–269.

Ourisson, G., Rohmer, M., 1992. Hopanoids. 2. Biohopanoids: a novel class of bacteria lipids. Accounts of Chemical Research 25, 403–408.

Ourisson, G., Rohmer, M., Poralla, K., 1987. Prokaryotic hopanoids and other polyterpenoid sterol surrogates. Annual Review of Microbiology 41, 301–333.

Overland, J.E., Adams, J.M., Mofjeld, H.O., 2000. Chaos in the North Pacific: spatial modes and temporal irregularity. Progress in Oceanography 47, 337–354.

Paffenhofer, G.-A., Van Sant, K.B., 1985. The feeding response of a marine planktonic copepod to quantity and quality of particles. Marine Ecology Progress Series 27, 55–65.

Parkes, R.J., Taylor, J., 1983. The relationship between fatty acid distributions and bacterial respiratory types in contemporary marine sediments. Estuarine, Coastal and Shelf Science 16, 173–189.

Perry, G.J., Volkman, J.K., Johns, R.B., Bavor, H.J., 1979. Fatty acids of bacterial origin in contemporary marine sediments. Geochimica et Cosmochimica Acta 43, 1715–1725.

Pfannkuche, O., 1993. Benthic response to sedimentation of particulate organic material at the BIOTRANS station, 47°N, 20°W. Deep-Sea Research II 40, 135–149.

Platt, T., Harrison, W.G., Lewis, M.R., Li, W.K.W., Sathyendranath, S., Smith, R.E., Vezina, .A.F., 1989. Biological production of the oceans: a case for a consensus. Marine Ecology Progress Series 52, 77–88.

Prahl, F.G., Eglinton, G., Corner, E.D.S., O' Hara, S.C.M., Forsberg, T.E.V., 1984. Changes in plant lipids during passage through the gut of *Calanus*. Journal of the Marine Biological Association of the UK 64, 317–334.

Prahl, F.G., Muehlhassen, L.A., Zahnle, D.L., 1988. Further evaluation of long-chain alkenones as indicators of paleoceanographic conditions. Geochimica et Cosmochimica Acta 52, 2303–2310.

Phleger, C.F., Nichols, P.D., Virtue, P., 1997. Lipids and buoyancy in southern ocean pteropods. Lipids 32, 1093–1100.

Ratmeyer, V., Fischer, G., Wefer, G., 1999. Lithogenic particle fluxes and grain size distributions in the deep ocean off northwest Africa: implications for seasonal changes of aeolian dust input and downward transport. Deep-Sea Research I 46, 1289–1337.

Rice, A.L., Billett, D.S.M., Fry, S., Johns, A.W.G., Lampitt, R.S., Mantoura, R.F.C., Morris, R.J., 1986. Seasonal deposition of phytodetritus to the deep-sea floor. Proceedings of the Royal Society of Edinburgh B 88, 265–279.

Rohmer, M., Bouvier-Nave, P., Ourisson, G., 1984. Distribution of hopanoid triterpenes in procaryotes. Journal of General Microbiology 130, 1137–1150.

Roman, M.R., Dam, H.G., Gauzens, A.L., Urban-Rich, J., Foley, D.J., Dickey, T.D., 1995. Zooplankton variability on the equator at 140°W during the JGOFS EqPac study. Deep Sea Research II 42, 673–693.

Saito, H., Murata, M., 1996. The high content of monoene fatty acids in the lipids of some midwater fishes: family myctophidae. Lipids 31, 757–763.

Sargent, J.R., 1976. The structure, metabolism and function of lipids in marine organisms. In: Malins, D.C., Sargent, J.R. (Eds.), Biochemical and Biophysical Perspectives in Marine Biology, Vol. 3. Academic Press, London, pp. 149–212.

Sargent, J.R., 1989. Ether-linked glycerides in marine animals. In: Ackman, R.G. (Ed.), Marine Biogenic Lipids, Fats, and Oils. CRC Press, Boca Raton, FL, pp. 176–193.

Sargent, J.R., Whittle, K.J., 1981. Lipids and Hydrocarbons in the Marine Food Web. Academic Press, London.

Siegel, D.A., Armstrong, R.A., 2002. Corrigendum to "Siegel, D.A, Deuser, W.G 1997: trajectories of sinking particles in the Sargasso Sea: modeling of statistical funnels above deep-ocean sediment traps deep-sea research I, 44, 1519–1541". Deep-Sea Research I, 49, 1115–1116.

Siegel, D.A., McGillicuddy Jr., D.J., Fields, E.A., 1999. Mesoscale eddies, satellite altimetry, and new production in the Sargasso Sea. Journal of Geophysical Research 104, 13359–13379.

Skerratt, J.H., Nichols, P.D., Bowman, J.P., Sly, L.I., 1992. Occurrence and significance of long-chain ($\omega-1$)-hydroxy fatty acids in methane-utilizing bacteria. Organic Geochemistry 18, 1989–1994.

Smith, C.R., Hoover, D.J., Doan, S.E., Pope, R.H., DeMaster, D.J., Dobbs, F.C., Altabet, M.A., 1996. Phytodetritus at the abyssal seafloor across 10° of latitude in the central equatorial Pacific. Deep-Sea Research II 43, 1309–1338.

Smith Jr., K.L., Baldwin, R.J., Karl, D.M., Boetius, A., 2002. Benthic community responses to pulses in pelagic food supply: North Pacific Subtropical Gyre. Deep-Sea Research I 49, 971–990.

Smith, R.C., Baker, K.S., 1985. Spatial and temporal patterns in pigment biomass and warm-core ring 82B and its environs. Journal of Geophysical Research 90, 8859–8870.

Steinberg, D.K., Carlson, C.A., Bates, N.R., Goldthwait, S.A., Madin, L.P., Michaels, A.F., 2000. Zooplankton vertical migration and the active transport of dissolved organic and inorganic carbon in the Sargasso Sea. Deep-Sea Research I 47, 137–158.

Steinberg, D.K., Carlson, C.A., Bates, N.R., Johnson, R.J., Michaels, A.F., Knap, A.H., 2001. Overview of the US JGOFS Bermuda Atlantic Time-series Study (BATS): a decade look at ocean biology and biogeochemistry. Deep-Sea Research II 48, 1405–1447.

Sweeney, E.N., McGillicuddy, D.J., Buesseler, K.O. Biogeochemical impacts due to mesoscale eddy activity in the Sargasso Sea as measured at the Bermuda Atlantic Time Series (BATS) site. Deep-Sea Research II, in press.

Teshima, S., Kanazawa, A., 1972. Bioconversion of β-sitosterol and 24-methyl-cholesterol to cholesterol in marine Crustacea. Comparative Biochemistry and Physiology B 39, 815–822.

Urrere, M.A., Knauer, G.A., 1981. Zooplankton fecal pellet fluxes and vertical transport of particulate organic material in the pelagic environment. Journal of Plankton Research 3, 369–387.

Versteegh, G.J.M., Bosch, H.-J., DeLeeuw, J.W., 1997. Potential palaeoenvironmental information of C_{24}–C_{36} mid-chain diols, keto-ols and mid-chain hydroxy fatty acids; a critical review. Organic Geochemistry 27, 1–13.

Vinogradov, M.E., 1962. Feeding of the deep-sea zooplankton. Rapport Proces et Verbeaux Réunion du Conseil international pour l'Exploraton de la Mer 153, 114–120.

Volkman, J.K., 1986. A review of sterol markers for marine and terrigenous organic matter. Organic Geochemistry 9, 83–99.

Volkman, J.K., Barrett, S.M., Dunstan, G.A., Jeffrey, S.W., 1992. C_{30}–C_{32} alkyl diols and unsaturated alcohols in microalgae of the class Eustigmatophyceae. Organic Geochemistry 18, 131–138.

Volkman, J.K., Barrett, S.M., Blackburn, S.I., Mansour, M.P., Sikes, E.L., Gelin, F., 1998. Microalgal biomarkers: a review of recent research developments. Organic Geochemistry 29, 1163–1179.

Wagner, D., 1999. Assessment of the probability of extreme weather events and their potential effects in large conurbations. Atmospheric Environment 33, 4151–4155.

Wakeham, S.G., 1987. Steroid geochemistry in the oxygen minimum zone of the eastern tropical North Pacific Ocean. Geochimica et Cosmochimica Acta 51, 3051–3069.

Wakeham, S.G., 1995. Lipid biomarkers for heterotrophic alteration of suspended particulate organic matter in oxygenated and anoxic water columns of the ocean. Deep-Sea Research I 42, 1749–1771.

Wakeham, S.G., Canuel, E.A., 1986. Lipid composition of the pelagic crab *Pleuroncodes planipes*, its feces, and sinking particulate organic matter in the equatorial North Pacific Ocean. Organic Geochemistry 9, 331–343.

Wakeham, S.G., Lee, C., 1993. Production, transport and alteration of particulate organic matter in the marine water column. In: Engel, M.H., Macko, S.A. (Eds.), Organic Geochemistry, Principles and Applications. Plenum Press, New York, pp. 145–165.

Wakeham, S.G., Lee, C., Farrington, J.W., Gagosian, R.B., 1984. Biogeochemistry of particulate organic matter in the oceans: results from sediment trap experiments. Deep-Sea Research 31, 509–528.

Wakeham, S.G., Hedges, J.I., Lee, C., Peterson, M.L., Hernes, P.J., 1997. Compositions and transport of lipid biomarkers through the water column and surficial sediments of the equatorial Pacific Ocean. Deep-Sea Research II 44, 2131–2162.

Williams, R.G., Follows, M.J., 2002. Physical transport of nutrients and the maintenance of biological production. In: Fasham, (Ed.), Ocean Biogeochemistry: a JGOFS Synthesis. Springer, Berlin.

Yano, Y., Nakayama, A., Yoshida, K., 1997. Distribution of polyunsaturated fatty acids in bacteria present in intestines of deep-sea fish and shallow-sea poikilothermic animals. Applied and Environmental Microbiology 63, 2572–2577.

Zedler, S., Yu, X., McNeil, J.D., Manov, D., Dickey, T., Sigurdson, D., Frye, D., Jannasch, H., Chang, G., 1997. Bermuda Testbed Mooring data report. Technical Report #OPL-5-97, University of California, Santa Barbara Ocean Physics Laboratory.

Zeng, Y.B., 1988. Geochemical studies of microbial lipids. Ph.D. Thesis, University of Bristol.

Zhang, X., Dam, H.G., 1997. Downward transport of carbon by diel migrant mesozooplankton in the central equatorial Pacific. Deep-Sea Research II 44, 2191–2202.